AD_____

AWARD NUMBER: W81XWH-05-1-0265

TITLE: Preclinical Mouse Models of Neurofibromatosis

PRINCIPAL INVESTIGATOR: Kevin Shannon, M.D.

CONTRACTING ORGANIZATION: University of California
San Francisco, CA 94143

REPORT DATE: October 2009

TYPE OF REPORT: Final

PREPARED FOR: U.S. Army Medical Research and Materiel Command
Fort Detrick, Maryland 21702-5012

DISTRIBUTION STATEMENT: Approved for Public Release;
Distribution Unlimited

REPORT DOCUMENTATION PAGE

Form Approved
OMB No. 0704-0188

1. REPORT DATE	2. REPORT TYPE	3. DATES COVERED
1 October 2009	Final	30 Sep 2005 – 29 Sep 2009

4. TITLE AND SUBTITLE

Preclinical Mouse Models of Neurofibromatosis

5a. CONTRACT NUMBER

5b. GRANT NUMBER
W81XWH-05-1-0265

5c. PROGRAM ELEMENT NUMBER

6. AUTHOR(S)

Kevin Shannon, M.D.

E-Mail: shannonk@peds.ucsf.edu

5d. PROJECT NUMBER

5e. TASK NUMBER

5f. WORK UNIT NUMBER

7. PERFORMING ORGANIZATION NAME(S) AND ADDRESS(ES)

University of California
San Francisco, CA 94143

8. PERFORMING ORGANIZATION REPORT NUMBER

9. SPONSORING / MONITORING AGENCY NAME(S) AND ADDRESS(ES)
U.S. Army Medical Research and Materiel Command
Fort Detrick, Maryland 21702-5012

10. SPONSOR/MONITOR'S ACRONYM(S)

11. SPONSOR/MONITOR'S REPORT NUMBER(S)

12. DISTRIBUTION / AVAILABILITY STATEMENT
Approved for Public Release; Distribution Unlimited

13. SUPPLEMENTARY NOTES

14. ABSTRACT

This report describes the past four years of research performed by a Consortium of investigators who were continuously funded by this Program since 1999 to develop, characterize, and utilize strains of mice that accurately model tumors found in persons with NF1 and NF2. This Consortium has generated many novel models of NF1 and NF2-associated tumors and has exploited these strains to investigate biologic and preclinical questions. The investigators have collaborated closely and have extensively shared expertise and reagents with each other and with NF researchers around the world. These mouse strains developed through this effort are a cornerstone of NF research and are instrumental to an effort by the Children's Tumor Foundation to organize and support a preclinical network for testing therapeutics that might benefit persons with NF1 and NF2 disease.

15. SUBJECT TERMS
Neurofibromatosis, benign tumors, cancer, mouse models

16. SECURITY CLASSIFICATION OF:			17. LIMITATION OF ABSTRACT	18. NUMBER OF PAGES	19a. NAME OF RESPONSIBLE PERSON
a. REPORT	b. ABSTRACT	c. THIS PAGE			19b. TELEPHONE NUMBER *(include area code)*
U	U	U	UU	45	USAMRMC

TABLE OF CONTENTS

INTRODUCTION

Benign and malignant tumors are a major cause of morbidity and mortality in individuals with NF1 and NF2. The *NF1* and *NF2* genes function as tumor suppressors in humans and mice. Although a great deal has been learned about the genetics, biochemistry, and cell biology of NF1 and NF2-associated tumors, it has proven difficult to translate these advances into new treatments. Accurate, well-characterized mouse models of NF-associated tumors are invaluable resources for achieving the long-term goal of bringing improved treatments to NF patients. The overall purpose of this consortium, which is now ending after 10 years, has been to develop such models that would serve as permanent resources for the scientific community. These efforts were timely for a number of reasons.

First, advances in gene targeting technologies in the late 1990s made it feasible to introduce many types of alterations into the mouse germline. Indeed, investigators who pioneered this general strategy were awarded the Nobel Prize in Medicine in 2007. The members of this research consortium developed the initial strains of *Nf1* and *Nf2* mutant mice, which provided major insights into a number of the complications seen in human NF1 and NF2 patients. Through this consortium effort, we engineered conditional mutant alleles of both *Nf1* and *Nf2* and in used these novel strains to create tractable new models for biologic and preclinical studies. Second, investigating cells from these *Nf1* and *Nf2* mutant mice has provided numerous fundamental insights that are directly relevant to understanding deregulated growth in *NF1* and *NF2*-deficient human cells. Genetic analysis of human and murine tumors has provided compelling evidence that *NF1/Nf1* and *NF2/Nf2* function as tumor suppressor genes (TSGs) *in vivo*. Biochemical studies of the proteins encoded by these genes (neurofibromin and merlin, respectively) furthered our understanding of how they regulate cell growth and revealed target proteins and pathways for rational drug design. The improved mouse models developed by this consortium also provide invaluable platforms for rigorous preclinical trials of these innovative approaches. Third, new therapies are urgently needed for many of the tumors that arise in individuals with NF1 and NF2. The current treatments for neurofibroma, optic nerve glioma, vestibular schwannoma, and for NF1 and NF2-asociated malignancies are frequently ineffective and carry a substantial risks of long-term morbidities. This consortium is highly complementary to the ongoing efforts of the NF Clinical Trials Consortium that is supported by this Program, which involve investigating novel treatments in NF patients, as the models that we have created facilitate testing novel agents and approaches in a controlled preclinical setting. These models are also integral to an ongoing initiative of the Children's Tumor Foundation to organize and support a preclinical network for testing therapeutics that might benefit persons with NF1 and NF2 disease. The quantity of drug required, expense, time to obtain data, and potential liability are all either greatly reduced or eliminated in mouse models. These strains therefore facilitate testing a wide range of new therapies that might benefit NF patients. Our work under this award focuses on the two overall technical objectives (aims) listed below.

(1) To enhance existing strains of *Nf1* and *Nf2* mutant mice and to develop new *in vivo* models of NF-associated tumors. We will fully characterize lesions that arise in these mice, focusing on how closely they reproduce the phenotypic, genetic, and biochemical alterations seen in comparable human tumors.

(2) To perform *in vitro* and *in vivo* studies to elucidate biochemical pathways underlying the proliferative advantage of *Nf1* and *Nf2*-deficient cells as a way of identifying molecular targets for therapeutic interventions.

These technical objectives included a series of studies that were organized under specific subheadings in our application. For clarity, this Final Report follows a similar format. Additional information can also be found in the many research publications supported by this award (see Reportable Outcomes section).

BODY

Background

Tumor Spectrum in NF1 and NF2 Patients. Persons with NF1 are predisposed to benign neurofibromas, optic nerve gliomas, and to specific malignant neoplasms. Individuals with NF1 typically develop multiple neurofibromas that can result in cosmetic, orthopedic, and neurologic disabilities. Optic nerve gliomas are another vexing clinical problem. Although histologically benign, these tumors frequently cause visual impairment or blindness because of their anatomic location. The malignant neoplasms seen in NF1 patients include astrocytoma, malignant peripheral nerve sheath tumor (MPNST), pheochromocytoma, and juvenile myelomonocytic leukemia (JMML). NF2 affects 1 in 40,000 persons worldwide. NF2 affects 1 in 40,000 persons worldwide. Individuals with NF2 develop schwannomas along cranial nerves (especially the eighth nerve), as well as peripheral nerves. Other NF2-related tumors include meningiomas, gliomas, and ependymomas.

Production and Characterization of *Nf1* and *Nf2* Mutant Mice. Drs. Jacks and Parada independently disrupted *Nf1* by inserting a neomycin *(neo)* cassette into exon 31 (1, 2). Homozygous *Nf1* mutant ($Nf1^{-/-}$) embryos die *in utero* with cardiac anomalies, which precluded the use of these mice to study important aspects of NF1 pathology, including the formation of many tumor types. To circumvent this problem, Dr. Parada's lab harnessed *Cre-loxP* technology to create a conditional *Nf1* allele (3). Importantly, the Parada's lab showed that the $Nf1^{flox}$ allele functions as a wild-type (WT) allele in spite of harboring *loxP* sites and a *neo* gene within its intronic sequences. The $Nf1^{flox}$ allele is readily recombined *in vivo* to make a null allele through co-expression of *Cre* recombinase. Drs. McClatchey, Jacks, and Giovannini used gene targeting to disrupt the *Nf2* locus (4, 5). Homozygous *Nf2* mutant embryos failed without initiating gastrulation. Although heterozygous *Nf2* mutant mice are cancer prone, these animals do not develop schwannoma or meningioma. To circumvent the early embryonic-lethal phenotype associated with homozygous inactivation of *Nf2* and to test the hypothesis that the tumor spectrum might be modulated by the rate of the loss of the normal allele in specific tissues, Dr. Giovannini and his colleagues generated a conditional mutant *Nf2* allele (6). As expected, mice homozygous for the $Nf2^{flox2}$ mutant allele ($Nf2^{flox2/flox2}$) were viable and fertile suggesting that the introduction of *loxP* sites did not hamper *Nf2* expression. Induced expression of *Cre* recombinase in $Nf2^{flox2/flox2}$ mice results in biallelic inactivation of *Nf2* in specific tissues. A major research goal of this Consortium has involved exploiting these conditional mutant alleles of *Nf1* and *Nf2* to develop tractable models of NF-associated tumors for use in our labs and by other investigators. We have made all strains available to academic investigators as soon as they were

published with no restrictions. A list of investigators who have received these mice appears in the Reportable Outcomes section.

Models of NF1 and NF2-Associated Tumors. In work published previously, the participants in this consortium reported the phenotypic and biologic features of NF1-associated mouse tumor models of MPNST/Triton tumor, astrocytoma, JMML, plexiform neurofibroma, and chemotherapy-induced leukemia, sarcoma, and breast cancer (7-12) and of NF2-associated tumors such as vestibular Schwannoma and meningioma (4, 5). These data are also described in detail in previous Progress Reports.

Functions of Neurofibromin and Merlin in Growth Control and Tumor Suppression. Work performed in our laboratories and by other NF investigators have begun to elucidate the normal biochemical functions of the proteins encoded by the *NF1* (neurofibromin) and *NF2* (merlin) genes.

Neurofibromin is a large protein that contains a catalytic GTPase activating protein domain, which greatly accelerates GTP hydrolysis on Ras proteins. These data led to a general model in which loss of neurofibromin leads to excessive Ras signaling in susceptible cells and that this, in turn, promotes tumor formation. This hypothesis, which is consistent with many studies of mouse and human tumors, has fundamental implications for treating the complications of NF1 disease as many pharmaceutical and biotechnology companies are actively developing and evaluating inhibitors of Ras effectors such as PI3 kinase, Akt, mTOR, Raf, and MEK as anti-cancer drugs.

Merlin is a member of a family of proteins that link membrane proteins to the underlying cortical actin cytoskeleton. Although its function is not as well understood as that of neurofibromin, most studies are consistent with a model in which merlin assembles signaling complexes beneath the plasma membrane and tethers them to certain membrane receptors thereby providing local regulation of receptor signaling. A number of studies have suggested that merlin can control the distribution of and signaling from the ErbB family of growth factor receptors, which have been implicated in many forms of human cancer. This is important because the development and analysis of therapeutic agents that target ErbB family members is currently a major effort in the field of cancer therapeutics.

Research Progress Report

Technical Objective (Aim) 1: To produce and characterize models of NF-associated tumors.

Loss of *Nf2* Cooperates with Oncogene Activation to Induce Adult-Onset Tumors Typical of NF2 Patients. Despite the clear association with *NF2* mutations, meningiomas and ependymomas have proven difficult to model in the mouse. Previous models of meningioma demonstrated relatively inefficient tumor initiation and/or limited tumor progression, and no mouse model of ependymoma has been developed to date.

Previous work from the Jacks lab on the developmental role of merlin suggests a potential mechanism that may underlie tumor initiation. In mice, asynchronous deletion of *Nf2* in early development results in widespread tissue fusion defects, including neural tube defects (13). The Jacks lab found that merlin is required for the assembly but not maintenance of junctional complexes in the nervous system, confirming *in vitro* studies (13). Therefore, in NF2 patients, loss of *NF2* function in a non-dividing cell with mature junctional complexes may have no adverse consequences. However, tumorigenesis may be initiated if that cell later re-enters the cell cycle and must assemble junctional complexes *de novo* (e.g. as a result of injury, oncogene activation, etc.) or if *NF2* loss occurs prior to tissue fusion. Indeed, there is evidence that injury may play a role in meningiomas since a history of head trauma significantly increases the risk of tumor development. In addition, the observation that ependymomas are particularly common in young children raises the possibility that the inciting event may be *NF2* loss in early development prior to neural tube closure.

The Jacks lab set out to develop a model of meningioma that would more closely mimic the timing and disease progression seen in patients. To do this, they deleted *Nf2* from adult meningothelial cells by delivering adeno-Cre intracranially through the skull of $Nf2^{fl/fl}$ mice. Mice were aged 10-67 weeks after infection (average 38 ± 16 weeks), and 4/28 developed small (0.23 ± 0.13 mm), low grade meningiomas or meningothelial hyperplasia at the injection site (**Fig. 1A**).

The Jacks lab hypothesized that an additional proliferative signal was required for efficient tumor induction. Therefore, they investigated whether oncogenic Ras can synergize with *Nf2* loss in meningioma formation. For this purpose, they used mice with conditional, constitutive activation of *Kras* from its endogenous promoter (*LSL-*$Kras^{G12D}$ mice). Following adeno-Cre administration, *LSL-*$Kras^{G12D}$; $Nf2^{fl/fl}$ (*K;Nf2*) mice developed large meningiomas (5.4 ± 3.5 mm), often distorting skull architecture and compressing brain structures similar to what has been observed in human patients (**Fig. 1B**; 12/17 treated mice). The majority of these tumors became evident 7-33 weeks after injury (average 25 ± 9 weeks), requiring the mice to be euthanized. Tumor histopathology closely mimicked that of grade I human meningioma including formation of whorls, psammoma bodies, and fascicular growth of spindle cells (**Figs. 1 and 2**). One tumor arose in a *K-*ras^{G12D}-only mouse following adeno-Cre administration (1/7). However, the histopathology of this tumor differed significantly from that seen in *Nf2* or *K;Nf2* mice and appeared to be of muscle rather than meningothelial origin. No tumors were detected in experimental mice that received vehicle alone (0/10), or in wild-type animals treated with adeno-Cre (0/5).

While most meningiomas in humans are benign, up to 20% demonstrate more aggressive histologic features and are characterized as “atypical” (grade II) or “anaplastic” (grade III) these tumors carry an increased risk of recurrence and a worse clinical outcome. In particular, patients diagnosed with anaplastic pathology (1-3% of all meningiomas) have a median survival of less than 2 years. Mutations in the *p16*^{Ink4a} and *p14*^{Arf} (*Ink4a/Arf*) tumor suppressors have been strongly associated with anaplastic meningiomas and to a lesser extent with atypical meningiomas. No pre-clinical models existed of these higher grade lesions. Therefore, the Jacks lab tested whether additional deletion of this locus using *p16*^{Ink4a}/*p19*$^{Arf\ fl/fl}$ mice in the *K;Nf2* mouse model would alter meningioma progression. Indeed, adult *K;Nf2;Ink4a/Arf* mice developed high grade, rapidly progressive meningiomas following adeno-Cre administration (**Fig. 1C**) with an average survival time of 16 ± 10 weeks post-injection (4/5 mice, 6.7 ± 3.1 mm). These tumors demonstrated many features of atypical or anaplastic meningiomas including high mitotic rate (>20 mitotic figures per 10 high power fields), areas of necrosis and large cell nuclei with prominent nucleoli (**Fig. 2D-F**). They also demonstrated brain invasion, an independent predictor of poor prognosis (**Fig. 1C**). Sheeting, a feature seen in atypical meningiomas, was common in both *K;Nf2* and *K;Nf2*;*Ink4a/Arf* mouse tumors following adeno-Cre injection (Fig. 2C). *Nf2;Ink4a/Arf* mice did not develop detectable tumors in this study (0/6).

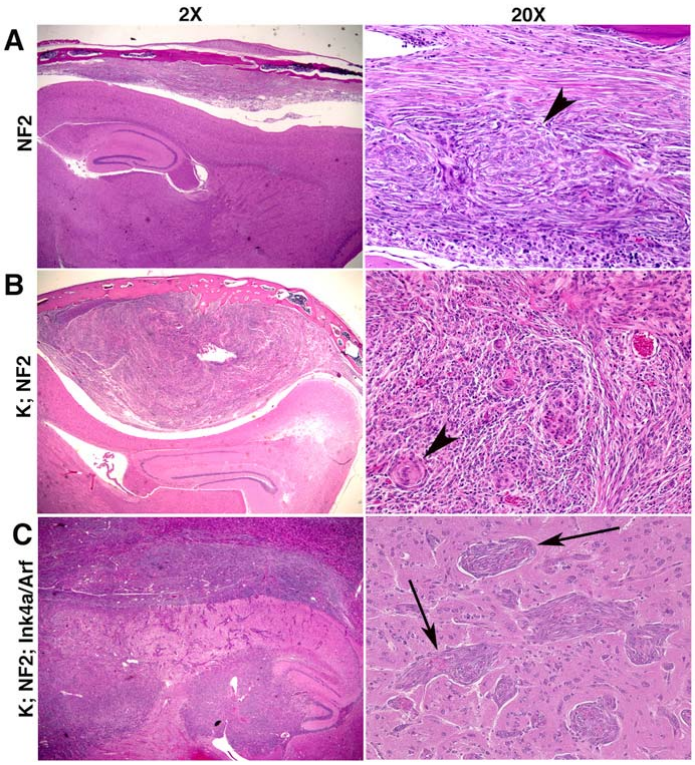

Figure 1. The full spectrum of meningioma histopathology can be modeled by Nf2 loss, K-ras activation, and Ink4a/Arf deletion
A small meningioma induced by adeno-Cre delivery through the skull of an adult Nf2$^{fl/fl}$ *mouse is shown in (A). When oncogenic K-ras*^{G12D} *is activated along with Nf2 deletion, large meningiomas form resulting in brain compression (B). These tumors demonstrate pathology typical of grade I meningioma including whorls (arrowheads A, B). By combining this model with deletion of the Ink4a/Arf tumor suppressor region, more aggressive tumors develop which directly invade and destroy brain tissue (C, arrows indicate nests of tumor cells within brain parenchyma). All samples were stained with hematoxylin and eosin and imaged at 20X or 200X original magnification as indicated.*

Given the robust induction of meningiomas from the combination of *Nf2* loss and *Kras*^{G12D} activation in the Jacks mouse model, the group investigated whether other NF2 phenotypes could also be modeled using this genetic combination. In particular, they sought to develop a model of cranial nerve schwannoma, as bilateral vestibular schwannomas are the most characteristic feature of NF2. Mice bearing a human glial fibrillary acidic protein *(hGFAP)* promoter driving Cre recombinase expression were used to conditionally activate *Kras*^{G12D} and/or delete *Nf2* from the cranial nerves. Expression from the *hGFAP* promoter lead to widespread recombination in the central nervous system beginning at embryonic day 13.5. *hGFAP-Cre;K;Nf2* mice exhibited extensive tumor formation in cranial nerves, particularly cranial nerve V, by 6 weeks of age. In addition, small nerve twigs that normally imperceptibly course through facial muscle were prominent and frequently contained tumor (data not shown). When 100 µm step sections were taken through the brains of these mice, the Jacks group identified small regions (<100 µm) of ependymal hyperplasia displaying rosettes. Such lesions did not appear to progress over time, although it was not possible to significantly age these mice. This was largely due to the development of two types of skin lesions: a severe dermatitis appearing around 6 weeks of age that required the mice to be euthanized; or large (1-2 cm) subcutaneous lesions containing cells that stained strongly positive for S100 (10/48 mice). These S100-positive lesions may represent dermal schwannomas, the most common type of skin tumor in NF2 patients. Both *Nf2* loss and *Kras*^{G12D} activation appeared to be required for these tumor phenotypes as 51 *hGFAP-Cre;NF2* mice aged for as long as 18 months revealed rare cases of dermatitis but no cranial nerve or subcutaneous tumors. *hGFAP-Cre;K* mice also did not develop skin or nervous system lesions (10 mice).

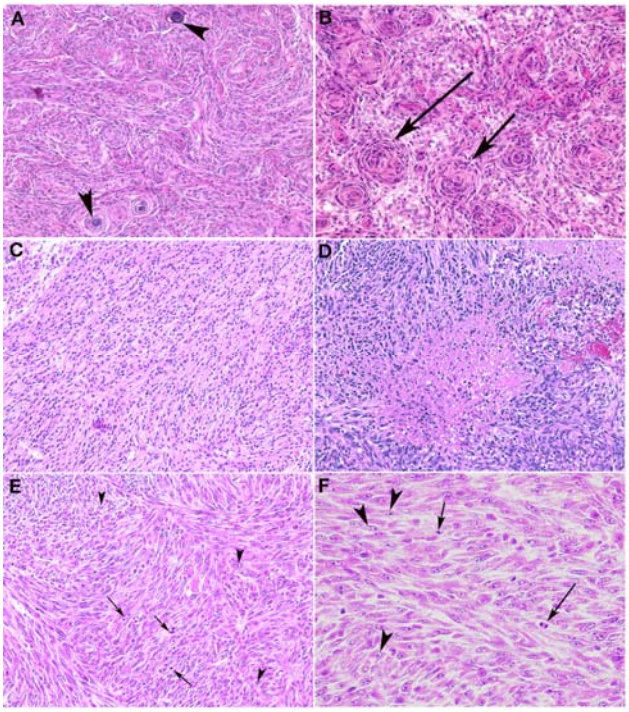

Figure 2. Histologic features of the mouse model of meningioma that recapitulate human meningioma
K;Nf2 mice recapitulated classic histopathologic features of grade I human meningioma including psammoma bodies (A, arrowheads), meningothelial whorls (B, arrows), and lobules of separated by collagenous septae (A, B). Certain features of human meningiomas have been associated with worse clinical outcome and higher WHO classification tumor grade. One of these features is sheeting, which was seen in meningiomas that developed in K;Nf2 mice (C), although the majority of the tumor had histopathology consistent with grade I transitional meningioma. When Ink4a/Arf deletion was introduced into this model, tumors not only displayed regions of sheeting but also spontaneous necrosis (D), frequent mitotic figures (arrows E, F) and large cell nuclei with prominent nucleoli (arrowheads E, F). Focal rhabdoid features were also seen in some K;Nf2;Ink4a/Arf tumors (E). All samples were stained with hematoxylin and eosin, panels A-E have an original magnification of 200X and F an original magnification of 400X.

A NF1 Mouse Model to Study Adult Onset Tumors. NF1 patients develop a range of tumors at different ages. Plexiform neurofibromas arise congenitally and involve multiple nerve fascicles, malignant peripheral nerve sheath tumors arise *de novo* or from malignant transformation of plexiform neurofibromas, and dermal neurofibromas arise during puberty or later in adulthood often in response to hormonal changes. These adult onset tumors are a particular concern for patients as they are often numerous, uncomfortable and disfiguring, even though they are typically benign by histology. While progress has been made in modeling congenital NF1 tumors, the mechanisms underlying the emergence of tumors in adulthood has been less certain. Data from existing models suggest that adult onset tumors require loss of the normal *NF1* allele during embryogenesis. However, they did not incorporate an *Nf1* heterozygous mutant background, which has been shown to be key to tumor development.

Therefore, the Jacks lab set out to determine whether neurofibromas could be initiated from cell types in the adult skin and nerve using the inducible Cre recombinase system in heterozygous *Nf1* mutant mice, which models the microenvironment seen in patient tumors. The Jacks lab generated tamoxifen-inducible Cre mice (Rosa26-CreER^{T2}) that permit local ablation at desired time points. This mouse model allowed careful control of the timing of *Nf1* loss by crossing Rosa26-CreER^{T2} mice with conditional $Nf1^{flox/+}$and $Nf1^{+/-}$ mice to generate Rosa26-CreER^{T2}; $Nf1^{flox/-}$ mice, with mice effectively being heterozygous *Nf1* mutant. *Nf1* is lost in sporadic cells following tamoxifen administration.

A Mouse Model of NF1-Associated Optic Glioma. To better characterize the etiology and development of optic glioma (pilocytic astrocytoma), the Parada lab has generated a mouse model of these tumors. Optic gliomas are benign tumors that affect ~25% of children with NF1. Although rarely life threatening, serious clinical complications can develop including loss of vision and physical intrusion on surrounding CNS structures resulting in endocrine complications. These tumors do not respond well to classic anti-tumor therapies, and surgical removal is difficult and has had limited success. Like other tumor types in the setting of NF1 sucn as plexiform neurofibroma and JMML, optic gliomas show a limited developmental window of opportunity for appearance. Optic gliomas primarily appear before age 6. Therefore, as in the other mentioned childhood NF1-associated tumors, it is suspected that a combination of either specific progenitor cells and/or microenvironment present during a particular timing of tissue development (in this case optic nerve) renders tumor susceptibility. Deletion of *Nf1* driven by a human *GFAP* promoter-driven Cre transgene causes optic nerve hyperproliferation and frank optic nerve tumors in a mouse model (14). When the *NF1* gene was differentially inactivated in specific cell types, loss of *NF1* in the optic nerve progenitors of the astrocytic lineage alone was insufficient to cause astrocytoma formation. Instead, either global heterozygosity (implicating the need for at least partial *Nf1* loss in other tissues) or loss in both the glial lineage and the neuronal lineage was required for tumors to appear (14-16). The potential role of retinal neurons lacking *Nf1* in contributing to tumor development and possible signaling mechanisms were explored.

Investigating the Role of Shh Signaling in *hGFAP-Cre; $Nf1^{fl/fl}$* Astrocytes. Little is known about the biology and development of optic pilocytic astrocytomas. To create mouse models that more closely mimic the disease observed in individuals with NF1, the Parada lab generated conditional mouse lines utilizing a *hGFAP* promoter to drive Cre recombinase and ablate *Nf1* expression from mice homozygous for the conditional mutant $Nf1^{fl}$ allele. In these mice, Cre is expressed

beginning at embryonic day 10.5 and results in loss of *Nf1* in developing progenitor cells in the central nervous system. The resulting mice have no neurofibromin expression in glial cells and some neurons (14). Analysis of optic nerves revealed significant hyperplasia of the astrocytes and 25% of the mice developed optic gliomas. These lesions are characterized by cellular disorganization, coarse fibrillary appearance and nuclear pleiomorphism, consistent with human stage I pilocytic astrocytomas (14). A second Cre-expressing transgene developed in David Gutmann's laboratory (*GFAP-Cre**; denoted by the asterisk*) uses a similar promoter with differences in the construct that result in *Nf1* loss only in astrocytes in the optic nerve and not in the retina or any of its cells. In addition, expression of this transgene appears less robust thus giving the impression of activating Cre recombinase at slightly later stages than the *hGFAP-Cre* transgene. Importantly, the Gutmann *hGFAP-Cre** mice have reduced potential to yield optic glioma formation (16). When this *GFAP-Cre** mouse is bred with the traditional *Nf1* knockout in heterozygous form ($Nf1^{fl/-}$) so that all cells in the mouse have only one copy of *Nf1*, hyperplasia (and some aspects of optic glioma formation) results, whereas when bred to the $Nf1^{fl/fl}$ mice such that cells not expressing the Cre recombinase are wild-type, no tumors develop (16). This requirement for a heterozygous environment supports the hypothesis that the loss of *Nf1* in astrocytes alone is insufficient for tumorigenicity. Instead, a non-cell autonomous signal may drive optic glioma formation.

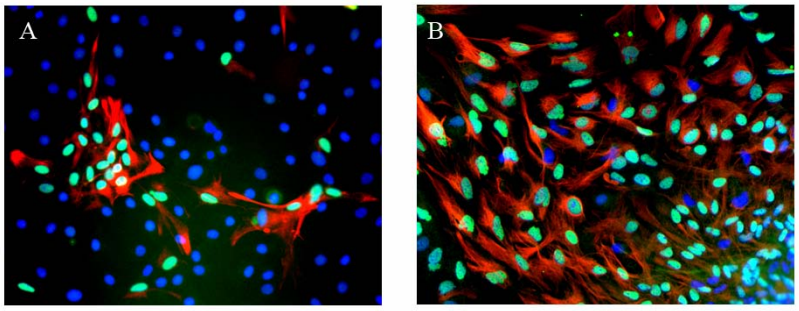

Figure 3. *Immunopanning results in pure astrocyte cultures. Cells prior to immunopanning (A) and post-immunopanning (B). Astrocytes are marked with GFAP (red) and Pax-2 (green). DAPI staining of cellular nuclei in blue.*

These observations suggest that the *Nf1*-deficient astrocytes have a growth advantage that is insufficient to drive tumor formation. In *GFAP-Cre;* $Nf1^{fl/fl}$ mice, astrocytes transiently proliferate abnormally throughout the CNS until P8, but only astrocytes in the optic nerve continue to proliferate and form optic gliomas (14). These observations indicate that either the astrocytes in these two areas are intrinsically different or that their relative microenvironments afford them different growth potentials after P8. To gain information about how the microenvironment in the optic nerve might drive *Nf1*-deficient astrocyte lineage cells to form tumors, a primary culture system where components of the system could be added and subtracted was used. A technique developed by the Barres laboratory to isolate astrocytes from rat optic nerves (17) was modified for this purpose: optic nerves from individual neonatal mouse pups (P1-P8) were microdissected and immunopanning was performed to isolate astrocyte lineage cells from the optic nerves of *GFAP-Cre;* $Nf1^{fl/fl}$ mice and littermate controls to >95% purity (**Fig. 3**).

Immature astrocytes isolated from the brains of *Nf1*-deficient mice exhibit a slight but reproducible proliferation advantage over wild-type astrocytes (16). A growth analysis of optic nerve astrocyte lineage cells comparing *GFAP-Cre;* $Nf1^{fl/fl}$ mice in the presence (knockout) and absence of *GFAP-Cre* (WT) was therefore performed. Astrocytes were isolated from both P1 mice, prior to the peak of astrocyte proliferation, and P8, after the peak of proliferation. Astrocytes lacking *Nf1* isolated from P1 mice had an early growth advantage *in vitro* (**Fig. 4, day**

3). This growth advantage was not noted at day 5, when cells became confluent in culture (**Fig. 4, day 5**). In contrast, in astrocytes isolated from P8 neonatal pups, astrocytes lacking *Nf1* do not exhibit a significant difference in proliferation in comparison to astrocytes lacking one copy of NF1 (heterozygous) or astrocytes with both copies of *Nf1* intact (data not shown). These results were confirmed by both manual counting of cells and by use of an ATP-based luminescence screen. A Cre recombinase-expressing adenovirus was utilized to perform these assays with *in vitro* deletion of *Nf1* and again, no significant growth advantage for *Nf1*-deficient astrocytes was observed (data not shown). These results are consistent with the *in vivo* observations of optic glioma formation in that loss of *Nf1* is not sufficient for prolonged abnormal astrocyte growth and tumorigenicity. In the absence of non-cell autonomous signals, which are present *in vivo*, the astrocytes from the optic nerve have an early, mild growth advantage, which is not sustained.

Since loss of *Nf1* in astrocytes alone is insufficient for optic glioma formation, a non-cell autonomous signal, derived from the surrounding microenvironment has been postulated to be required for glioma formation. One candidate signaling molecule that is expressed by retinal ganglion cells (RGCs) is Sonic hedgehog (Shh). Previous expression studies demonstrated both Shh mRNA and protein expression in RGCs, but only protein expression in the optic nerve (18). Immunohistochemistry (IHC) studies using specific antibodies confirmed the presence of Shh protein in the projections of the RGCs and in the optic nerve (not shown). Expression of patched (Ptch), the receptor for Shh, was also observed in the optic nerve, as well as in the Müller cells in the inner nuclear layer. The expression of Shh signaling components in the *GFAP-Cre; Nf1$^{fl/fl}$* mice was therefore examined. These mice lack *Nf1* expression in astrocytes and precursor cells within the optic nerve, as well as in RGC (14). To assess Shh signaling in this mouse model, the expression patterns of Ptch and Gli2, one of the zinc-finger transcription factors activated by Shh signaling, was examined. Gli2 is induced in cells that receive Shh signaling (19). When *Nf1* is selectively ablated by expression of Cre recombinase, the expression of both Ptch and Gli2 in the optic nerve is increased as compared to control mice with normal expression of *Nf1* (**Fig. 5**). These results indicate that in the absence of *Nf1*, there is up-regulation of Shh signaling components.

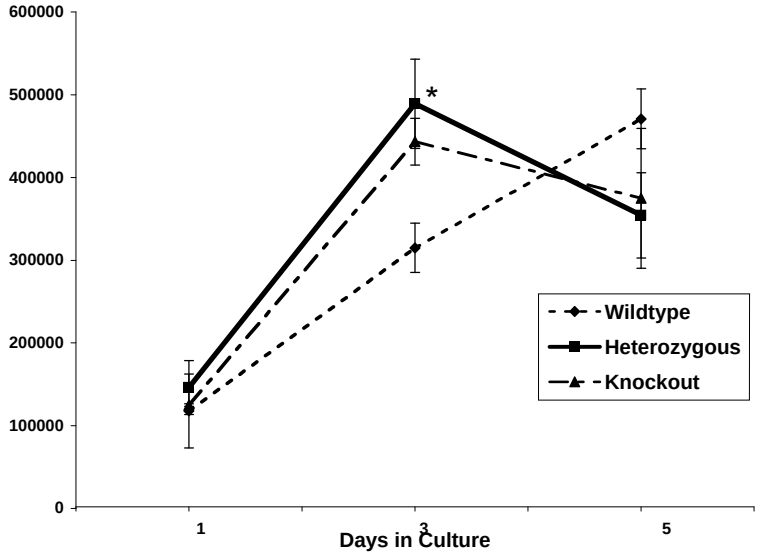

***Figure 4**. Nf1-deficient astrocytes show an early growth advantage when isolated from P1 optic nerves. Astrocytes were isolated at P1 from individual optic nerves via immunopanning. Resultant cultures were maintained for 7-10 days and then plated in duplicate for growth analysis. Growth analysis was performed using Promega Cell-Titer Glo Luminescent Cell Viability Assay on days 1, 3 and 5 post plating. *P<0.05. All points with SEM.*

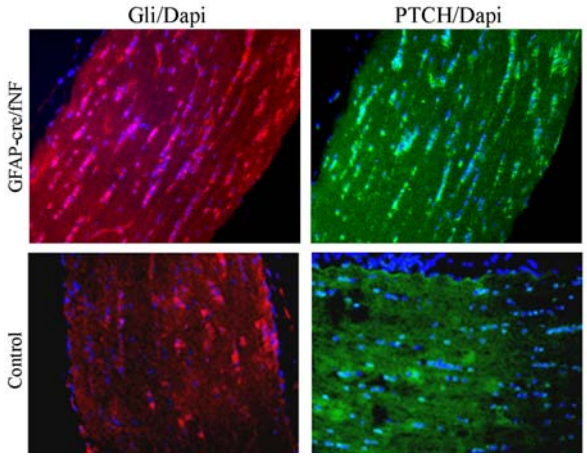

Figure 5. *Optic nerves deficient in Nf1 have higher levels of patched and Gli2 than control optic nerves. Optic nerves were dissected from 3-month-old mice, fixed and paraffin embedded. 5 micron sections were generated and IHC performed with anti-Gli antibody (in red) and anti-Patched (in green). Blue is DAPI nuclear staining. Top two panels derived from GFAP-Cre-fNf1 mice. Bottom two panels from age-matched littermate controls.*

Previous work has shown that inhibition of Shh *in vivo* leads to a decrease in the number of astrocytes in the optic nerve (18). These data, along with the expression analysis results described above, led the Parada lab to determine the effect of blocking Shh signaling on the proliferation of WT, $Nf1^{+/-}$, and $Nf1^{-/-}$ astrocytes *in vitro*. The cells were treated with cyclopamine, a *Veratrum* alkaloid that specifically inhibits Shh signaling by binding to and blocking Smoothened, a requisite component of the receptor complex (20). They found that inhibiting Shh signaling caused a statistically significant decrease in proliferation in astrocytes lacking one (heterozygous) or both (knockout) copies of *Nf1* (**Fig. 6**). Therefore, the Parada lab has shown that Shh may play an important role in the proliferation of astrocytes in the optic nerve, especially in the context of loss of *Nf1*. This mouse model of optic glioma developed by the Parada lab provides an excellent preclinical model for testing inhibitors of Shh as well as other novel therapies.

<u>Plexiform Neurofibromas and the Microenvironment</u>. Interactions between tumorigenic cells and their surrounding microenvironment are critical for tumor progression, but are not fully understood. Genetic studies indicate that biallelic loss of *Nf1* is required in the tumorigenic cell of origin in the embryonic Schwann cell lineage. However, loss of heterozygosity is insufficient for neurofibroma formation, and *Nf1* haploinsufficiency in at least one additional non-neoplastic lineage is required for tumor progression. The

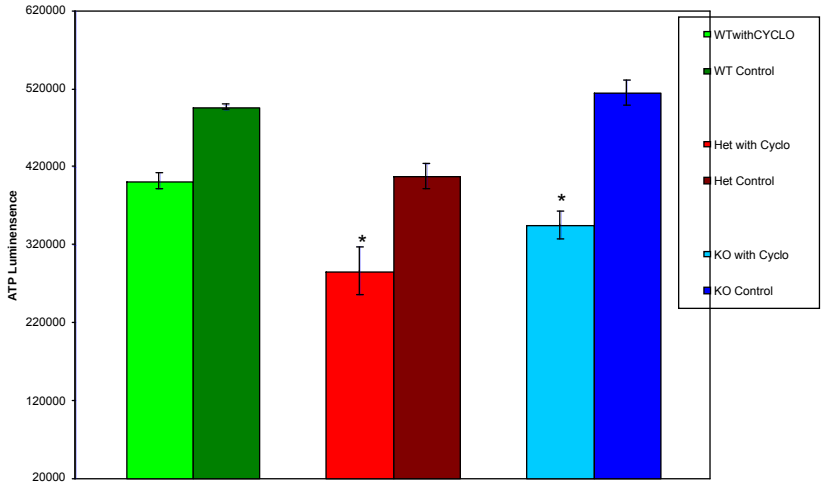

Figure 6*. Blocking Shh signaling with cyclopamine inhibits growth of astrocytes lacking one or both copies of Nf1. Astrocytes were isolated from P1 optic nerves via immunopanning, grown in culture for 7-10 days and then plated in duplicate. Cyclopamine (10 mg/mL), an inhibitor of Shh signaling, was added to individual wells (or an equal amount of DMSO as a control). Cells were then assayed at day 5 via the Promega Cell-Titer Glo Luminescent Cell Viability kit. Green: wild-type astrocytes; Red: Nf1 heterozygous astrocytes; Blue: Nf1-deficient astrocytes.*

Parada lab, in collaboration with the laboratories of Wade Clapp and David Ingram, has made strides toward unraveling the contributions of the microenvironment to plexiform neurofibroma development in NF1. They demonstrated that *Nf1* heterozygosity in bone marrow, in the context of Schwann cell progenitor *Nf1* nullizygosity, is required to allow neurofibroma development and progression (21). Through a series of bone marrow transfers of normal marrow into tumor-prone mice, and of *Nf1* heterozygous marrow into non-tumor-prone mice, they conclusively demonstrated a requisite interaction between *Nf1* nullizygous Schwann cell progenitors and *Nf1* heterozygous bone marrow. Further studies have allowed them to conclude that it is the heterozygous mast cells in the donor bone marrow that cooperate with nullizygous Schwann cell lineage cells to promote tumor formation. Moreover, either genetic or pharmacologic inhibition of the mast cells is sufficient to block tumor formation and surprisingly to reduce tumor burden in the mice (21). Most importantly, mast cells in the hematopoietic lineage were identified as the critical interactors in tumor development. These studies have now been extended to the clinic (clinical trials are currently underway) with preliminary data that suggest a possible strategy to treat these tumors with imatanib, a potent inhibitor of mast cells. Attenuating the microenvironmental contribution to tumor development thus affords the best new hope for an effective treatment for these previously untreatable tumors.

Malignant Peripheral Nerve Sheath Tumors (MPNSTs). The Parada lab previously combined conditional mutant alleles of *Nf1* and *Tp53* to model MPNST. These studies were hampered by the fact that when *Tp53* was mutated, not only did this lead to appearance of MPNSTs, but also to other *Tp53*-associated malignancies that caused mortality. The Parada Lab next developed mice with a *cis* $Nf1^{fl/-};Tp53^{fl/+}$ genotype, which required enormous effort because *Nf1* and *Tp53* are closely linked on mouse chromosome 11. The resultant mice when crossed to *Krox20-Cre* mice developed plexiform neurofibromas at earlier ages than previously observed with mutation of *Nf1* alone (12). Moreover, *cis* $Nf1^{fl/-};Tp53^{fl/+}$ mice developed MPNSTs within the plexiform tumors. This result was exciting because it suggests that the issue of unrelated *Tp53* tumor formation has been overcome, allowing focus on the development of the MPNSTs. However, this proved to be overly optimistic as the mice rarely developed sufficiently large MPNSTs prior to death because the plexiform tumors were so large.

Dermal Neurofibromas and Skin-Derived Precursors. Freda Miller and her colleagues pioneered the discovery and study of a novel progenitor cell found in the dermis. These cells, termed skin-derived precursors or SKPs, are present in humans and rodents, are apparently broadly accessible from skin, and exhibit properties of neural progenitors when cultured *in vitro* (22). More specifically, these cells resemble cells of neural crest lineage, and indirect studies have provided evidence for a possible neural crest origin. Moreover, in elegant studies, Miller and colleagues have demonstrated the capacity of SKPs to differentiate into Schwann cells *in vivo* in mouse strains that are deficient for myelin (23).

The Parada lab became interested in SKPs after noting that SKPs were localized to the appropriate region and had cellular properties that made them suitable candidates for the cell of origin of dermal neurofibromas. They therefore set out to investigate whether in fact SKPs could be the cell of origin for dermal neurofibromas. They isolated SKPs from the dermis of mice using the Miller group protocols and grew them in suspension cultures with standard media used to culture neural stem cells from the CNS (24). In a series of validation studies again following the Miller group, they showed that their SKP cultures exhibited a similar surface marker profile

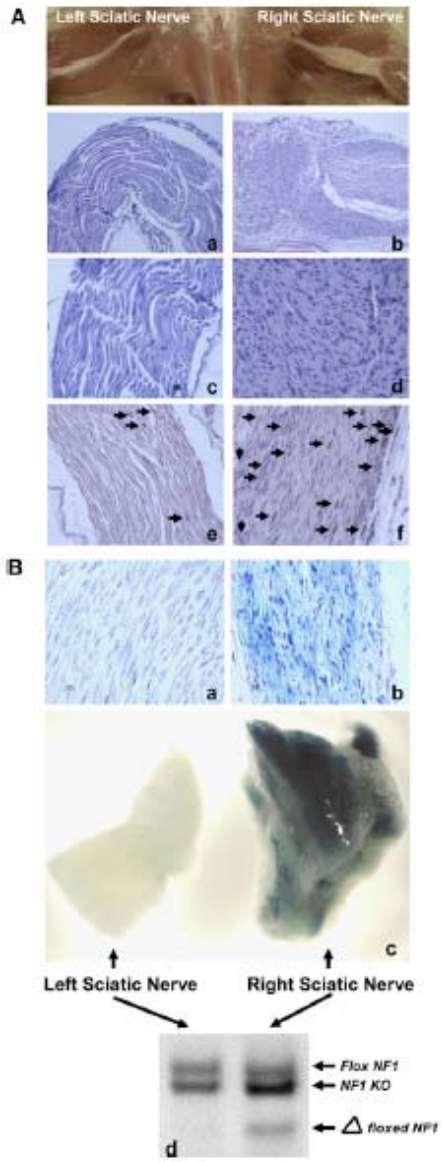

Figure 7. *SKPs were purified from skin of CMV-CreERT2;Nf1flox/-;ROSA26 mice and exposed to tamoxifen to induce recombination at the ROSA26 and Nf1 loci. Two to three months after SKP implantation, mice were perfused with 4% paraformaldehyde and left and right sciatic nerves were harvested for X-gal staining of whole nerves. The nerves were then post-fixed in formalin for paraffin sectioning and counter-stained with nuclear fast red. X-gal stainings of whole left and right sciatic nerves show that the enlarged right sciatic nerve is X-gal positive (**c**, right panel) but not the control left sciatic nerve (**c**, left panel). Paraffin sections show histological evidence of neurofibroma with X-gal-positive, disordered spindle-cell morphology, with ovoid and spindle-shaped nuclei for the right sciatic nerve (**b**) but not the control left sciatic nerve (**a**). The left and right sciatic nerves were also subjected to qPCR genotyping (**d**). The recombined loxP sites (floxed Nf1) at the Nf1 locus were detected in the tumor on the right sciatic nerve (**d**), further indicating that the neurofibromas are derived from the implanted SKPs. (Flox Nf1 = floxed Nf1 allele; Nf1 KO = mutant Nf1 allele).*

to adult neural stem cells derived from the dentate gyrus and the subventricular zone of the brain, specifically nestin and GFAP. They also confirmed that SKPs generate neurons and glia in culture. Armed with the adapted cultures, they set about testing their hypothesis that SKPs are the source of dermal neurofibromas. To obtain $Nf1^{-/-}$ SKPs, *CMV-CreER*^{T2} transgenic mice were crossed with $NF1^{fl/-}$*;Rosa26* mice to generate *CMV-CreER*^{T2}*;*$NF1^{fl/-}$*;Rosa26* mice. The CMV promoter is active in most cell types and the ER^{T2} cassette provides the flexibility to induce Cre recombinase activity *in vitro* or *in vivo*. Finally, the *Rosa26* transgene permits tracing the SKPs at various times after manipulation. Skin was harvested from the backs and necks of these mice, SKPs isolated according to established protocols, and then exposed to 4OH-tamoxifen to activate the CreER^{T2} recombinase and generate $Nf1^{-/-}$*;LacZ+* SKPs. The effectiveness of recombination was monitored by LacZ staining as well as by PCR-based verification that the LoxP sites had been recombined (not shown; (25)). $Nf1^{-/-}$*;LacZ+* SKPs were then implanted back into the same animal as an autograft to avoid immunological rejection and to maintain a heterozygous *Nf1* mutant microenvironment. In these early experiments, when the SKPs were implanted intradermally or subcutaneously, no neurofibroma formation was observed over the course of seven months (data not shown). One possible explanation for failure of tumor engraftment might be technical, caused by ineffective association of the mutant SKPs with terminal peripheral nerve projections. This possible explanation arose from the knowledge that in the vast majority of cases, neurofibromas are always closely associated with peripheral nerves. In the context of plexiform neurofibromas, the sciatic nerve is a common site of tumor development. SKPs were therefore next reimplanted into the sciatic nerves of the same animals, where close proximity to the nerve could be achieved, to test the idea about nerve association. These autologously transplanted $Nf1^{-/-}$*;LacZ+* SKPs uniformly gave rise to sciatic plexiform neurofibromas within two

months post implantation, whereas transplanted *Nf1*$^{+/-}$ SKPs showed no signs of tumor growth (**Fig. 7**, and (26)). The neurofibromas exhibited the characteristics of human plexiform neurofibromas, being poorly circumscribed, composed primarily of spindle cells, and expressing the Schwann cell marker S100b. Excess collagen deposition and heavy infiltration of mast cells into these plexiform neurofibromas, a critical component of tumor initiation that is commonly observed in human neurofibromas, was also observed (12, 21, 27). Furthermore, LacZ staining of the tumors provided proof that the reimplanted SKPs themselves formed the tumor rather than inducing resident (LacZ negative) cells to form the tumors (**Fig. 7**). These exciting results provided preliminary data in support of the following hypotheses: (1) SKPs can give rise to neurofibromas; and, (2) the microenvironment in the sciatic nerve dictates plexiform rather than dermal tumors. Thus in all likelihood, the dermis microenvironment exerts control over the fate of dermal tumors.

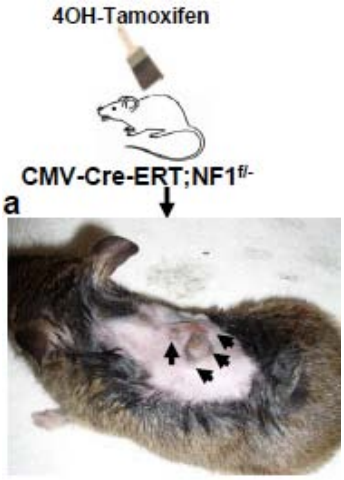

Figure 8. *Tamoxifen (TMX) was painted topically onto the upper back skin of neonatal CMVCreERT2;Nf1flox/- mice twice a day for 5 consecutive days. Six to seven months post tamoxifen application, these mice developed cutaneous nodules similar to human dermal neurofibroma at the TMX application sites. (from Le et al. 2009)*

To test more directly whether SKPs are the natural source of dermal neurofibromas, the Parada lab painted tamoxifen directly onto the shaved skin of mice could penetrate and reach SKPs in their natural environment. Using the *CMV-CreER*^{T2}*;Rosa26* mice painted with tamoxifen, SKPs were isolated and tested for LacZ staining. The results showed that this method of tamoxifen application could reach endogenous SKPs and induce recombination as assayed by isolation of SKPs from the tamoxifen treated skin and LacZ staining. They next applied tamoxifen to neonatal *CMV-CreER*^{T2}*;Nf1*$^{flox/-}$ mice, on the back and neck skin to ablate *Nf1* expression in SKPs *in vivo*. Six to seven months post tamoxifen application, cutaneous nodules similar to human dermal neurofibromas were observed at the application site (**Fig. 8**). These tumors were subjected to thorough histopathological analysis, including H&E staining, S100β expression as well as other markers of Schwann cells, and Leder staining for mast cell infiltration. The results indicated that these nodules were, by all criteria, dermal neurofibromas. These results further provided evidence that the cells of origin for dermal neurofibromas reside locally in the skin, since under the tamoxifen painting protocol, neurofibromas only developed at the site of application on the back and not at distant sites. Thus, these data point to SKPs, or their derivatives, as the source of NF1-associated dermal neurofibromas. Experiments now underway provide support for the idea that loss of *Nf1* in SKPs is required but not sufficient to induce tumors. These studies to date, to be further developed in future experiments, implicate an essential role for the tumor microenvironment, including neurons and hormones in neurofibroma development.

<u>MPNSTs Derived from SKPs</u>. MPNSTs frequently arise from plexiform neurofibromas and are invasive and incurable. To ask if SKPs can give rise to MPNST, SKPs mutant for both *Nf1* and *p53* were tested for their ability to generate neurofibromas. Skin was harvested from the backs of *cis NF1*$^{fl/fl}$*;Tp53*$^{fl/fl}$ mice, SKPs were isolated, and then exposed *ex vivo* to adenovirus carrying

Cre and GFP to ablate *Nf1* and *Tp53* expression and obtain *Nf1*$^{-/-}$;*p53*$^{-/-}$ SKPs. *Nf1*$^{-/-}$;*p53*$^{-/-}$ SKPs were then implanted back into the same animal subcutaneously as an autograft (**Fig. 9**). The Parada lab observed tumor formation within one month following transplantation (**Fig. 9**). This tumor appearance preceded normal *Nf1*-mediated dermal neurofibroma formation by many months. Subcutaneous transplantation of the *cis Nf1*$^{-/-}$;*p53*$^{-/-}$ SKPs into nude mice accelerated tumor formation to 6-8 weeks (not shown). Histological characterization of these tumors revealed a high mitotic index, high nuclear/cytoplasm ratio and invasion into the subcutaneous muscle layer. All of these properties are indication of malignant neoplasms that are not found in neurofibromas. Abundant melanin pigmentation within the tumor was also observed, a feature previously described in the original MPNST mouse model (28) and consistent with the idea that these tumors are of neural crest (melanocyte or Schwann cell) origin. Using IHC to phenotype these malignant tumors, they were seen to be S100 positive, further confirming their neural crest origin. They are also positive for the Schwann cell markers PLP, Sox10 and GAP43 (**Fig. 10**), validating that these tumors are MPNSTs. In summary, these experiments effectively induce MPNSTs from neural crest-derived stem/progenitor cells, indicating that an additional mutation in the *Tp53* tumor suppressor gene is required to predispose *Nf1*$^{-/-}$ mouse neural crest-derived cells to malignant transformation. As such, this novel model would be a useful for delineating molecular pathogenesis for clinical therapeutic studies in NF1-associated MPNST. These tumors can be readily generated without the confounding effect of *Tp53* associated malignancies and upon further validation, may be an ideal model for the detailed molecular characterization of these MPNSTs, as well as a source for high-throughput studies with small chemical compounds and with RNAi screens.

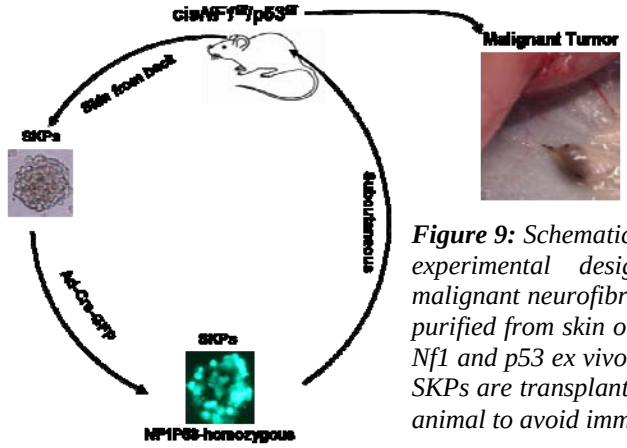

Figure 9: *Schematic representation of the experimental design to generate a malignant neurofibroma model. SKPs are purified from skin on back for ablation of Nf1 and p53 ex vivo. The cis p53-/-;Nf1-/- SKPs are transplanted back into the same animal to avoid immunorejection.*

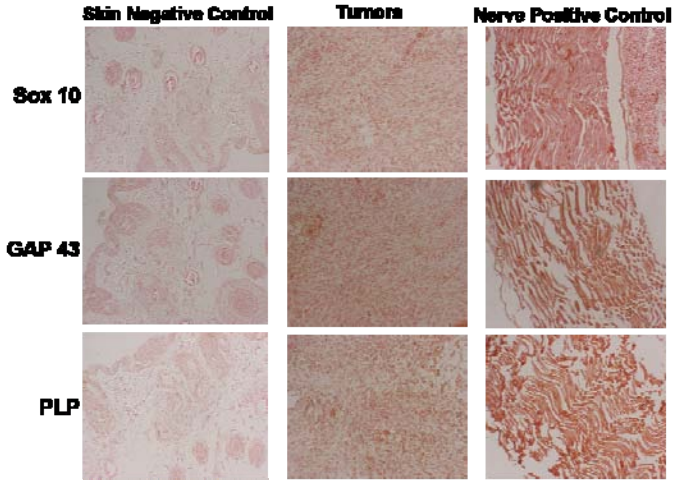

Figure 10: *Analysis of tumor derived from Nf1*$^{-/-}$*;p53*$^{-/-}$ *conditional mutant SKPs. Anti-Schwann cell markers Sox10, GAP43, and PLP immunohistochemistry followed by Nuclear Fast red counterstain.*

Use of Heterozygous *Nf1* Mutant Mice to Model A Spectrum of Secondary Malignant Neoplasms (SMNs). Nearly two thirds of cancer patients, including many with NF1, receive radiation therapy. Modern treatment protocols typically involve administering a high dose of fractionated irradiation to a defined anatomic site of disease. Retrospective studies have shown that the vast majority of SMNs arise in tissues that were included in the radiation field and support a relationship between the total dose of radiation and tumorigenesis. Previous murine studies of radiation mutagenesis have generally employed single, low dose total body irradiation (TBI) to promote tumors. In both mice and humans, TBI is delivered in limited doses, which does not accurately model the high dose targeted radiotherapy most cancer patients receive. Understanding the relationship between radiation dose and late complications could inform current efforts to reduce late risks. This is particularly relevant in persons with NF1 as retrospective clinical data suggest that treatment with genotoxins for a primary cancer markedly ncreases the risk of common SMNs such as myeloid leukemia and soft tissue sarcoma (29, 30)

Based on these clinical observations and on the lack of robust animal models of SMN, the Shannon lab administered either the alkylating agent cyclophosphamide (CY), a single dose of total body irradiation (TBI), or both genotoxins to heterozygous *Nf1* mutant mice ($Nf1^{+/-}$) (7, 9). When delivered alone or in combination with cyclophosphamide, TBI induced a spectrum of SMNs in $Nf1^{+/-}$ mice that included myeloid malignancies, soft tissue sarcomas, and breast carcinomas. Interestingly, a single low dose of TBI (3 Gy) cooperated more strongly with *Nf1* inactivation than six doses of cyclophosphamide (7). However, low dose TBI does not accurately model current radiation oncology practice. To address this important limitation, the Shannon lab collaborated with Dr. Jean Nakamura (Department of Radiation Oncology, UCSF) to develop a customized technique to model clinical brain radiotherapy, which is responsible for a high proportion of SMNs in cancer survivors. This novel procedure allowed us to deliver focal, fractionated cranial irradiation (CI) to WT control and $Nf1^{+/-}$ mice according to a dose and schedule that closely replicates current treatment protocols (**Fig. 11A**). Similar to the whole brain irradiation technique used in patients, equally weighted, opposed lateral beams were used to deliver multi-fraction CI. Radiographic film was used to quantitate radiation dosimetry, describing the absolute radiation dose rate both within and outside the irradiation field and the dose homogeneity across the beam aperture at varying tissue depths (**Fig. 11B**).

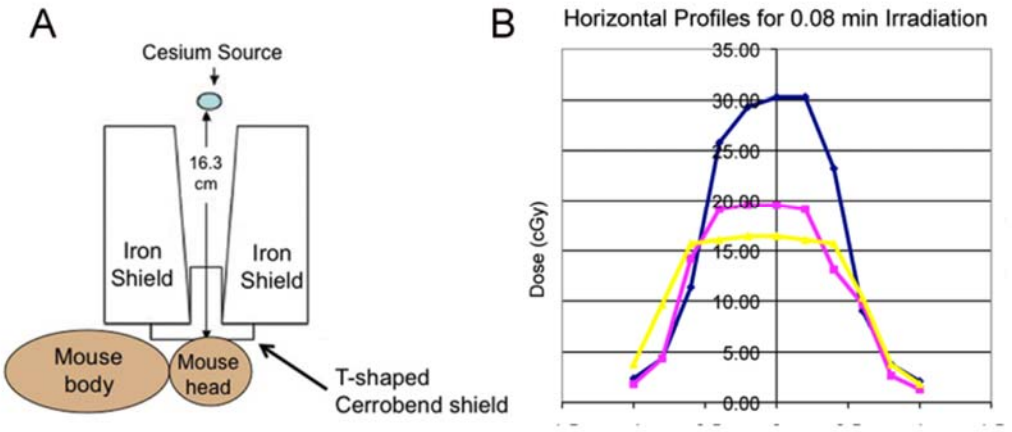

Figure 11. CI set-up and dosimetry. ***A.*** *Schematic cross-section through the cesium-137 irradiation device depicting the irradiation set up and the relationship of the animal to the source. The mouse's body, eyes, ears and throat are spared from irradiation by iron and cerrrobend shields. The beam aperture measures 1 cm (0.5 to -0.5 cm on the figure).* ***B.*** *The horizontal profiles of the dose rate in air (no buildup), at 1 mm tissue depth (0.1 cm buildup), and at 1 cm tissue depth (1 cm buildup) were measured with calibrated radiographic film.*

As expected from previous reports (1, 2, 7, 9), the survival of unirradiated *Nf1*$^{+/-}$ mice was reduced compared to WT littermates with deaths occurring after one year of age (**Fig. 12A**). CI significantly decreased the survival of both WT and *Nf1*$^{+/-}$ mice (**Fig. 12A**). Due to the uniform survival of unirradiated WT mice (**Fig. 12A**), the magnitude of this difference was greater in the WT group (p=0.002 versus p=0.05 in *Nf1*$^{+/-}$ mice). However, the median post-treatment survival time was reduced in irradiated *Nf1*$^{+/-}$ mice compared to irradiated WT mice (503 versus 596 days; p =0.04), showing that the worst overall survival was observed in irradiated *Nf1*$^{+/-}$ mice. Interestingly, the survival of WT and *Nf1*$^{+/-}$ mice was reduced to a similar extent by either moderate dose (3 Gy x 5) or high dose (3 Gy x 10) CI (**Fig. 12B**).

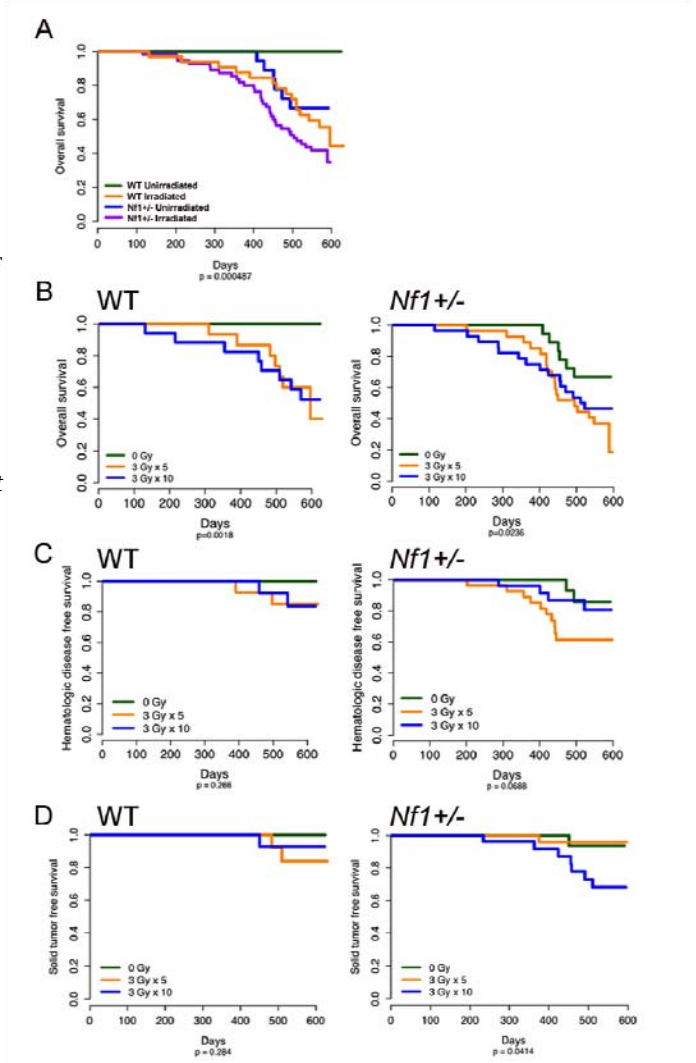

Figure 12*. Survival and Disease-Specific Survival after CI in WT and Nf1+/- Mice**. *Kaplan-Meier survival curves depict overall survival, solid tumor free survival, and hematologic disease free survival in WT and Nf1 mutant mice. Log-rank tests were used to test for differences between survival curves. The latency to death was measured from the date of the last radiation treatment.* ***A and B. *Both WT and Nf1 mutant mice had decreased survival after CI.* ***C.*** *Kaplan-Meier cause-specific survival curves were generated to describe death due to hematologic or solid tumor diseases. Nf1 mutant mice exposed to 15 Gy CI were significantly more likely to die of hematologic disease than Nf1 mutant mice that were unirradiated or exposedto 30 Gy CI (p=0.04).* ***D.*** *Nf1 mutant mice exposed to 30 Gy CI were significantly more likely to die of solid tumor than Nf1 mutant mice that were unirradiated or exposed to 15 Gy CI (p=0.04).*

.

Necropsies of moribund and terminally sacrificed mice revealed two major disease phenotypes; solid tumors within the irradiated region (in-field tumors) and myeloid malignancies. Dr. Nakamura performed log-rank tests to compare disease-specific survival due to myeloid malignancy and observed a trend for myeloid malignancies to be increased in *Nf1* mutant mice receiving 15 Gy of CI **(Fig. 12C)**. Disease-specific survival due to solid tumor was significantly reduced in *Nf1* mutant mice receiving 30 Gy of CI (**Fig. 12D**). The latency before the onset of clinical signs that necessitated euthanasia was similar in mice that died with solid tumors and myeloid malignancies.

Mice treated with CI developed several types of solid tumors arising from the central nervous system, bone, skin, and orbits within the irradiated region. These in-field solid tumors included squamous cell carcinomas, osteosarcoma, MPNST, papillary carcinoma, pituitary adenomas, choroid plexus papilloma, and lymphomas. Myeloid malignancies were diagnosed and characterized by examining the spleen, liver, sternum, and peripheral blood of affected animals. Importantly, the most common myeloid malignancy observed in irradiated *Nf1*$^{+/-}$ mice resembled human myelodysplastic syndrome (MDS), which is a common SMN in human patients.

The F1 strain background of this study cohort allowed the use of polymorphic markers to screen tumors for loss of constitutional heterozygosity (LOH). Molecular analysis uncovered three general patterns in the study cohort: LOH involving *Nf1*, LOH at the *Nf1* and *Tp53* loci, and absence of LOH (data not shown). *Nf1* inactivation was common in some tumor types, and infrequent on others. Previously described radiation-induced breast cancers and sarcomas generated by TBI were also analyzed at D11Mit31 and D11Mit219 microsatellites and at SNP rs13481119. Losses of *Nf1* and *Trp53* on the C57Bl/6-derived allele was common in these histologies, with the pattern of microsatellite and SNP losses implicating a chromosomal region spanning *Nf1* and *Trp53* on the C57Bl/6-derived allele. In contrast to the solid tumors, *Nf1* inactivation was uncommon in radiation-induced myeloid malignancies with only 2 of 12 splenic DNA samples showing LOH at *Nf1*.

Together, these data showing that focal radiation therapy and heterozygous *Nf1* inactivation cooperate strongly in tumorigenesis underscore the risk of radiation therapy in persons with NF1 and support the current clinical practice of only administering radiotherapy when absolutely necessary. Ongoing studies in the Nakamura and Shannon labs include characterizing Ras signaling in radiation-induced tumors and cell lines and testing the efficacy of targeted small molecule inhibitors in these models.

Technical Objective (Aim) 2: Consequences of Nf1 and Nf2 Inactivation and Therapeutic Target Identification

Merlin-Dependent Regulation of ErbB Signaling in Schwann cells (SCs). Published work from the McClatchey lab suggests that merlin can coordinate the process of adherens junction stabilization with silencing of the epidermal growth factor receptor (EGFR), thereby mediating contact-dependent inhibition of proliferation (31, 32). The McClatchey group has shown that loss of *Nf2* yields several different types of tumors in mice and that pharmacological inhibitors of the epidermal growth factor receptor (EGFR) halt the over-proliferation of $Nf2^{-/-}$ cells *in vitro* and *in vivo*. A major conclusion of these studies is that merlin controls the membrane distribution of and signaling from EGFR. Ongoing work in the McClatchey lab aims to delineate the molecular basis of how merlin controls receptor distribution. Follow-up studies suggest that primary $Nf2^{-/-}$ SCs also fail to undergo contact-dependent inhibition of proliferation and that this is dependent upon the presence of neuregulin (Nrg), the major mitogenic growth factor for SCs and the ligand for ErbB2:3 receptors (Schwann cells normally express very little EGFR). In fact, immunoprecipitation experiments revealed a marked increase in ErbB2:3 heterodimers in $Nf2^{-/-}$ SCs, consistent with the notion that this major SC mitogenic signaling complex is overactive (**Fig. 13**). Subsequent studies revealed that $Nf2^{-/-}$ SCs exhibit markedly increased levels of ErbB3 but not ErbB2, suggesting that deregulation of ErbB3 is central to the overproliferation of $Nf2^{-/-}$ SCs. This was supported by the observation that shRNA-mediated knockdown of ErbB3 rescues contact-dependent inhibition of proliferation in $Nf2^{-/-}$ SCs (**Fig. 15C**).

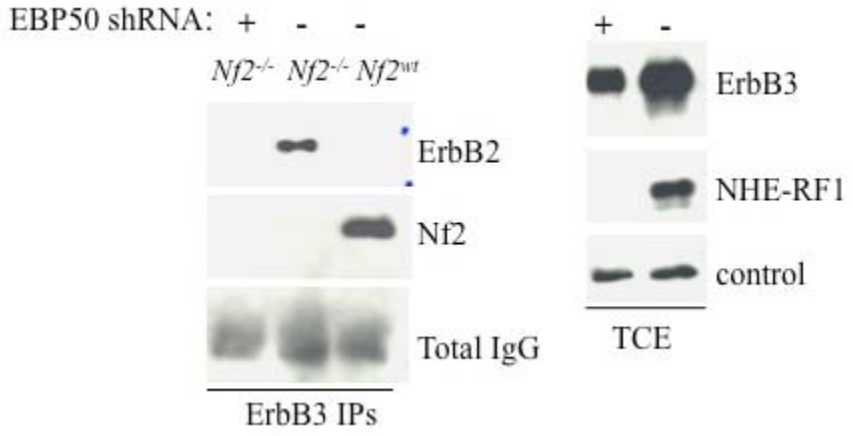

***Figure 13**: Immunoprecipitation of ErbB3 from wild-type and $Nf2^{-/-}$ SCs reveals a marked increase in ErbB2:ErbB3 dimerization in the absence of Merlin (left). shRNA-mediated knockdown of NHE-RF1 levels eliminates this ErbB2:3 dimerization and yields an decreased level of total ErbB3 (right).*

After observing increased ErbB3 levels in other types of primary $Nf2^{-/-}$ cells, the McClatchey lab set out to understand the molecular basis of the increased ErbB3 levels exhibited by $Nf2^{-/-}$ SCs. They measured equivalent levels of ErbB3 and ErbB2 mRNA in wild-type and $Nf2^{-/-}$ SCs, suggesting that the differences arose posttranslationally (**Fig. 14A**). They next examined ErbB3 stability in the presence and absence of merlin and found that ErbB3 levels remained higher in the $Nf2^{-/-}$ SCs in the presence of cyclohexamide, which blocks the synthesis of new protein; this suggests that Merlin controls the stability of ErbB3 (**Fig. 14B**). In contrast, SCs expressing

Merlin exhibit lower levels of total ErbB3, which are further reduced in the presence of cyclohexamide. Additional work suggested that this increased stability reflects protection from proteasome-mediated degradation (not shown). Preliminary studies suggest that merlin mediates ErbB3 stability by controlling its distribution to sterol-rich membranes – a model that fits well with their ongoing studies of merlin and EGFR.

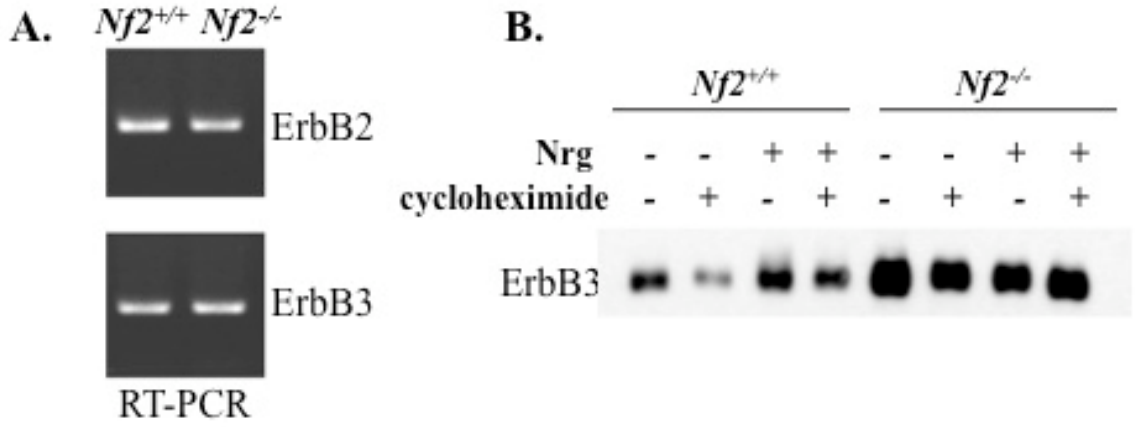

Figure 14**: Merlin controls ErbB3 stability.* ***A. *The levels of ErbB2 and ErbB3 mRNA were similar in wild-type and $Nf2^{-/-}$ SCs; however, the levels of ErbB3 protein were higher in the $Nf2^{-/-}$ SCs.* ***B.*** *Cyclohexamide treatment yielded a further decrease in ErbB3 levels in the wild-type SCs in the presence and absence of Nrg. In contrast, cyclohexamide had little effect on the high levels of ErbB3 in $Nf2^{-/-}$ SCs.*

Role of NHE-RF1 in Merlin-Mediated Regulation of ErbB3 Distribution and Signaling. The McClatchey group found that endogenous merlin and ErbB3 co-immunoprecipitate in SCs, prompting an investigation of the basis of how merlin associates with ErbB3. They focused on the PDZ-domain containing adapter NHE-RF1 that can associate with EGFR and is required for the association between Merlin and EGFR (31, 33). In fact, Dr. McClatchey's group noted that the reported NHE-RF1-interacting site(s) in EGFR are conserved in ErbB3 but not in ErbB2 or ErbB4; they have generated a virus expressing a version of ErbB3 in which those residues have been mutated to test this. The importance of NHE-RF1 was underscored by the observation that knockdown of NHE-RF1 prevents the excess ErbB3 levels and ErbB2:ErbB3 dimerization seen in $Nf2^{-/-}$ SCs and rescues contact-dependent inhibition of proliferation of $Nf2^{-/-}$ SCs (**Fig. 13, 15B**). Moreover, they found that NHE-RF1 levels are regulated by both cell density and Nrg such that they are exceedingly high in confluent, Nrg-bathed $Nf2^{-/-}$ SCs. Finally, they found that the levels of NHE-RF1 and ErbB3 are interdependent; thus shRNA-mediated knockdown of ErbB3 but not ErbB2 results in a dramatic reduction in NHE-RF1 levels. These studies reveal NHE-RF1 as a central player in merlin-dependent regulation of both EGFR and ErbB3, and therefore of combinatorial ErbB signaling. Ongoing studies aim to define the functional relationship between Merlin, NHE-RF1 and ErbB3.

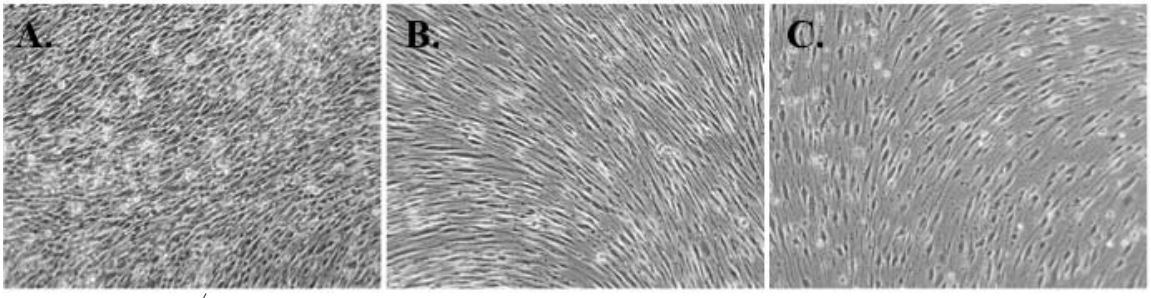

Figure 15. A. *$Nf2^{-/-}$ SCs grown in the presence of Nrg fail to undergo contact-dependent inhibition of proliferation and pile up on top of one another. Expression of shRNAs directed against NHE-RF1 (**B**) or ErbB3 (**C**), led to a restoration of contact-dependent inhibition of proliferation.*

<u>$Nf2^{-/-}$ SCs alter ErbB expression in the absence of Nrg</u>. Importantly, the McClatchey group has also found that SCs that are cultured in the absence of Nrg or injected subcutaneously (away from a source of Nrg), up-regulated EGFR and down-regulated ErbB3 at the transcriptional level, apparently to compensate for the lack of Nrg. For example, while parental $Nf2^{-/-}$ SCs exhibit undetectable levels of pEGFR, 5/5 subcutaneous tumors derived from the same cells show appreciable levels of pEGFR. Subcutaneous tumors derived from $Nf2^{-/-}$ SCs also show increased EGFR mRNA and decreased ErbB3 mRNA, as do some SC lines that have been established in the absence of Nrg. These observations have obvious implications regarding the preclinical use of xenograft models and regarding potential mechanisms of resistance to ErbB2-targeted therapies in NF2. Drs McClatchey and Giovannini are currently working together to determine whether this phenomenon is unique to mouse $Nf2^{-/-}$ SCs and to delineate its molecular basis.

<u>Generation of an Expanded-Mutant Strain of Mice</u>. Expanded is a FERM domain-containing protein that physically and genetically interacts with merlin in the fruitfly *Drosophila* (34). Recent studies in the fly suggest that Expanded and merlin, together function upstream of the Hippo/Salvador/Warts/Yki pathway(35). The McClatchey lab identified and cloned the putative mammalian orthologue of Expanded and generated antibodies that recognize the mammalian protein, which colocalizes with Merlin at cell:cell junctions and, like merlin, co-immunoprecipitates with the junctional protein E-cadherin. To generate a valuable tool for delineating the molecular function of mammalian Expanded and to investigate the function of Expanded in tumorigenesis, Dr. McClatchey's lab designed and engineered a conditional mutant allele of mouse *expanded*. This allele was successfully homologously targeted to the endogenous expanded locus in ES cells; however, the subsequent analysis of mice generated from these ES cells suggested that the allele was functioning as a severely hypomorphic or neomorphic allele due to the presence of a promoterless β-geo cassette embedded within an intron. This cassette was successfully removed via Flp-mediated recombination and the resulting ES cells used to regenerate chimeric animals. Chimeras were generated and bred to wild-type C57Bl/6J mice to yield constitutionally heterozygous conditional mutant animals that are viable and fertile (**Fig. 16**). These mice have now been crossed to *EIIa-Cre* mice in which the Cre recombinase is expressed in the early zygote, yielding removal of the cassette and the establishment of heterozygous null animals. The McClatchey group is currently intercrossing these $Ex^{+/-}$ mice to generate homozygous null embryos/animals ($Ex^{-/-}$), which will be analyzed in order to define the developmental requirements for Ex function. Cells from $Ex^{lox/lox}$ embryos have also been generated and will be infected with *Ad-Cre* to

***Figure 16**: Generation of mice that are heterozygous for a conditional Expanded mutant allele. PCR of tail DNA from 8 siblings derived from chimeric $Exp^{lox/+}$ ⇔wild-type X wild-type parents reveals the expected 50% transmission of the conditional mutant allele.*

generate *Ex* null cells for *in vitro* analyses. The antibody generated against mouse Expanded will be used to confirm loss of the protein in $Ex^{-/-}$ cells and tissues. Future studies include aging $Ex^{+/-}$ animals to monitor for cancer development, crossing *Ex*- and *Nf2*-mutant mice and targeting *Ex*-deficiency to tissues in which Merlin function is particularly important (ie the liver, kidney, Schwann cells) in order to approach the original goal of delineating the molecular relationship between Merlin and Expanded in mammals.

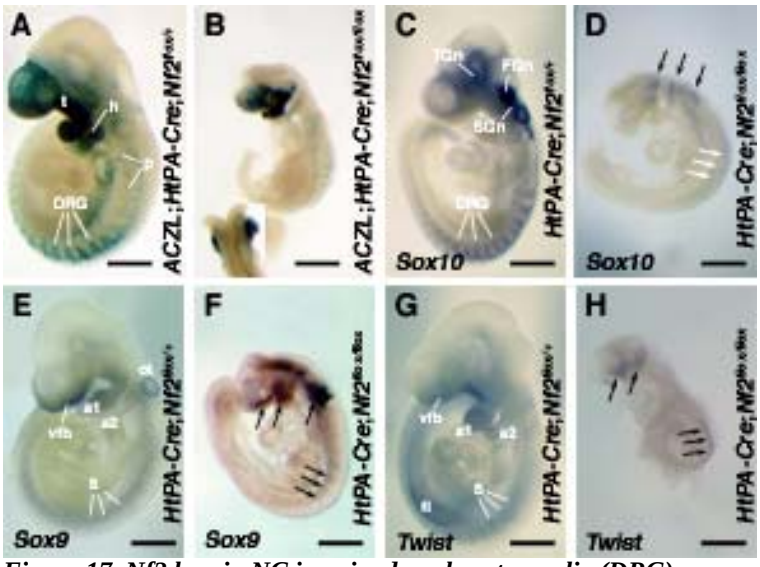

***Figure 17. Nf2 loss in NC impairs dorsal root ganglia (DRG) formation.** Cell-fate mapping by ß-Gal and Sox10 gene expression showing a strong reduction of NC cells in the trunk of HtPA-Cre;$Nf2^{flox2/flox2}$ embryos and suppression of DRG formation. (A-B) ß-Gal activity was revealed in $ACZL^{+}$;HtPA-Cre;$Nf2^{flox2/+}$ and $ACZL^{+}$;HtPA-Cre;$Nf2^{flox2/flox2}$ embryos by X-Gal staining. (A) At E9.5, the trigeminal (t), the hyoid (h) and the post-otic (p) NC streams were labelled in the cephalic region. In the trunk region, NC cells colonizing the somites that will give rise to the DRG, were labelled. (B) In mutant embryos, the trigeminal stream was as intense as in the WT embryo, while in the trunk there was a strong reduction of cells presenting the ß-Gal activity. (C-D) Sox10 expression was detected by mRNA whole mount in situ hybridization. (C) In control HtPA-Cre;$Nf2^{flox2/+}$ embryos, expression of Sox10 was restricted to NC cells giving rise to cranial and spinal sensory ganglia. In the cephalic region the trigeminal (TGn), the facial (FGn) and the superior (SGn) ganglia expressed Sox10. In the trunk, Sox10 was expressed in the DRG. (D) In HtPA-Cre;$Nf2^{flox2/flox2}$ embryos, Sox10 expression was reduced in the trunk region (white arrows), mirroring the ß-Gal staining pattern of $ACZL^{+}$;HtPA-Cre;$Nf2^{flox2/flox2}$ embryos. In the cephalic region, clusters of cells expressing Sox10 were present (black arrows), but their organization could not be traced back to that of control embryos. (E-H) Nf2 loss in NC did not change the expression of Sox9 and Twist. (E) In conrol HtPA-Cre;$Nf2^{flox2/+}$ embryos Sox9 was expressed in the ventral forebrain (vfb), in the first branchial arch (a1), at the edge of the otic placodes (ot) and in the somites (S). (F) In HtPA-Cre;$Nf2^{flox2/flox2}$ embryos the expression of Sox9, highlighted by arrows, covered that of control embryos. (G) In HtPA-Cre;$Nf2^{flox2/+}$ embryos twist expression was observed in the ventral forebrain, in the first and second (a2) branchial arches, in the somites and in the forelimbs (fl). (H) In HtPA-Cre;$Nf2^{flox2/flox2}$ embryos twist expression covered that of the control embryos. Bar is 0.5 mm.*

<u>Effects of *Nf2* Loss in Different Embryonic Tissues</u>. Dr. Giovannini and collaborators have investigated whether the developmental stage of neural crest-derived cells (NC) may determine susceptibility to *Nf2* loss. Merlin is required for early embryonic development. $Nf2^{-/-}$ mouse embryos die shortly after the onset of gastrulation due to defects in the epithelial organization of the extra-embryonic ectoderm (5). Spatially-controlled loss of *Nf2*, by driving Cre recombnase expression under the control of tissue-specific promoters, allows to overcome this early embryonic lethality (6, 13, 36). The Jack's lab previously analyzed the role of *Nf2* at early stages of mouse development using a *Nestin-Cre* (*NesCre*) transgene. In *NesCre* transgenic mice, mosaic

Cre expression was found in the neural tube and its derivatives, such as neuronal and glia precursor cells. *NesCre*;*Nf2*$^{flox/flox}$ embryos presented detachment-induced apoptosis at the open edge of the closing neural tube, and defaults of edges fusion during neurolation attributable to the lack of junctional complexes in *Nf2*$^{-/-}$ mutant neural tubes (13). More recently, the McClatchey lab has shown that inactivation of *Nf2*^{flox} alleles in the visceral endoderm driven by a specific *Villin-Cre* transgene induced an important lethality ranging from E17 to postnatal day 3. About 10% of the *Villin-Cre*;*Nf2*$^{flox/flox}$ surviving pups developed kidney neoplasia (36). These data show that, depending on the site and time, *Nf2* inactivation could either be pro-apoptotic or promote cell proliferation. Since some manifestations of NF2 disease can be imputed to neural crest defects, the Giovannini lab inactivated *Nf2* in developing neural crest cells. The *HtPA-Cre* transgenic driver line has proven to be a powerful tool for tissue-specific gene deletion in neural crests (37). In contrast to the *NesCre* line, the *Ht-PA-Cre* line does not target the central nervous system and therefore renders it more specific for NC cells. NC-specific deletion of the *Nf2* gene leaded to a specific set of developmental defects that are distinct from those of *NesCre*;*Nf2*$^{flox/flox}$ mutants. While the vast majority of *NesCre*;*Nf2*$^{flox/flox}$ embryos exhibited a global tissue fusion defect, but survived until birth (13), *HtPA-Cre*;*Nf2*$^{flox/flox}$ mutants showed patterning defects of the neural crest, leading to increased apoptosis and embryonic lethality. E9.5 *HtPA-Cre*;*Nf2*$^{flox2/flox2}$ embryos showed intense apoptosis at the open-edge of the neural tube in the cephalic region. This region contains cells not directly affected by *Nf2* loss in this model (**Fig. 17A, 17B, and 18G**), suggesting that apoptosis was induced indirectly due to the failure of neural tube fusion. *HtPA-Cre*;*Nf2*$^{flox/flox}$ mutant embryos also showed a significant reduction of NC cells, most likely by apoptotic processes, resulting in a size reduction as they started to shrink at E9.5, presumably at the beginning of NC cell migration. The complete degradation of mutant embryos was achieved by E15.5, when almost all *HtPA-Cre*;*Nf2*$^{flox2/flox2}$ yolk sacs were empty. Altogether, these differences can be attributed to the substantial Cre expression pattern differences in *NesCre* and *HtPA-Cre* transgenic mice (37, 38). Besides apoptosis at the open edges of the neural tube, *HtPA-Cre*;*Nf2*$^{flox2/flox}$ mutant embryos selectively activated the apoptosis program in the Cre-expressing mesenchyme of the trunk (**Fig.**

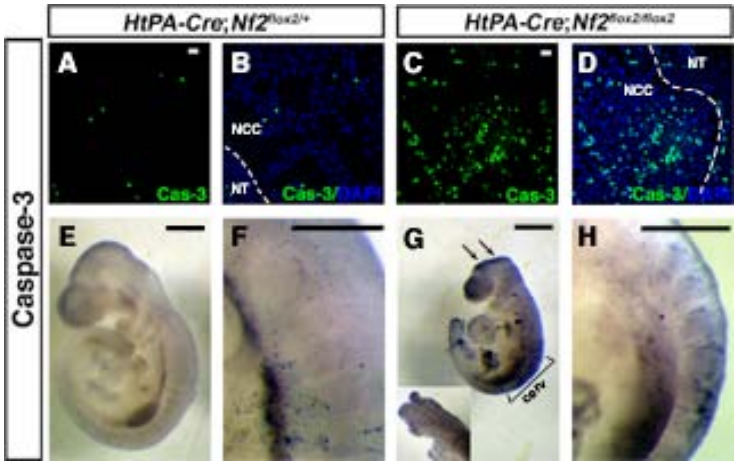

Figure 18. Enhanced apoptosis of Nf2$^{-/-}$ NC cells. *(A-D) The active form of the protease Caspase-3 (Cas-3), a marker for apoptotic cells, showed that NC cell cultures obtained from HtPA-Cre;Nf2$^{flox2/flox2}$ explants were more susceptible to apoptosis than HtPA-Cre;Nf2$^{flox2/+}$ control cultures. (A and B) Nf2$^{+/-}$ NC cultures had no cells in apoptosis. (C and D) A considerable amount of Nf2$^{-/-}$ NC cells were positive to Cas-3. (E-H) Whole mount immunochemistry aimed to detect activated Caspase-3 showed that in vivo apoptotic cells accumulated at the edges of the open neural tube and in the entire cervical region of the trunk. (E) At E9.5, control embryos expressed Cas-3 only in the dorsal aorta. (G) In the mutant embryos, arrows highlight the accumulation of apoptotic cells. Abbreviations: NCC, neural crest cells; NT, neural tube. In panels A-D the bar is 100 µm and in E-H the bar is 0.5 mm.*

18H). This was also reflected *in vitro* in the post-migratory NC cell cultures of neural tubes explants, suggesting a causal role of *Nf2* loss for the induction of apoptosis in these cells.

<u>*Nf2* Loss Does Not Affect NC Motility *in vitro*</u>. The function of merlin is regulated by Rac1, a small GTPase of the Rho family (39). Rac1 plays a major role in the control of the NC cell proliferation and its inactivation in NC induces their exit from the cell cycle once they have settled in the target organ. Intriguingly, *Rac1*$^{-/-}$ NC cells did not show obvious morphological changes when outgrowing from a neural tube explant *in vitro*. In contrast, *Nf2*$^{-/-}$ NC cells showed a substantial increase of filopodial protrusions reminiscent of Rho GTPase activation (40). Despite the dramatic morphological changes, the migration pattern of NC cells, at least their outflowing from neural tube explants, was not affected in this culture system. Although a relevant migration default was not observed in *Nf2*$^{-/-}$ NC *in vitro*, it cannot be excluded that the reduction of *Sox10* expression, as well as the numeric reduction of NC cell observed in the *PlpGFP*;*HtPA-Cre*;*Nf2*$^{flox2/flox2}$ and *ACZL*;*HtPA-Cre*;*Nf2*$^{flox2/flox2}$ embryos (**Fig. 17**), could be linked to an impairment of cell motility contributing to NC survival defects.

<u>Massive Apoptosis Starting in the Trunks of *HtPA-Cre*;*Nf2*$^{flox/flox}$ Embryos</u>. In addition to its association to tumor development, little is known about the role of *Nf2* in regulation of normal tissue homeostasis *in vivo*. In *NesCre*;*Nf2*$^{flox/flox}$ embryos, as an effect of *Nf2* loss, the edges of a closing neural tube fail to fuse and undergo anoikis (13). In a similar way, the Giovannini lab. observed intense apoptosis in E9.5 *HtPA-Cre*;*Nf2*$^{flox2/flox2}$ embryos at the open-edge of the neural tube in the cephalic region, an embryonic area that is not directly effected by *Nf2* loss in this model (**Figs. 17A, 17B and 18G**). It is

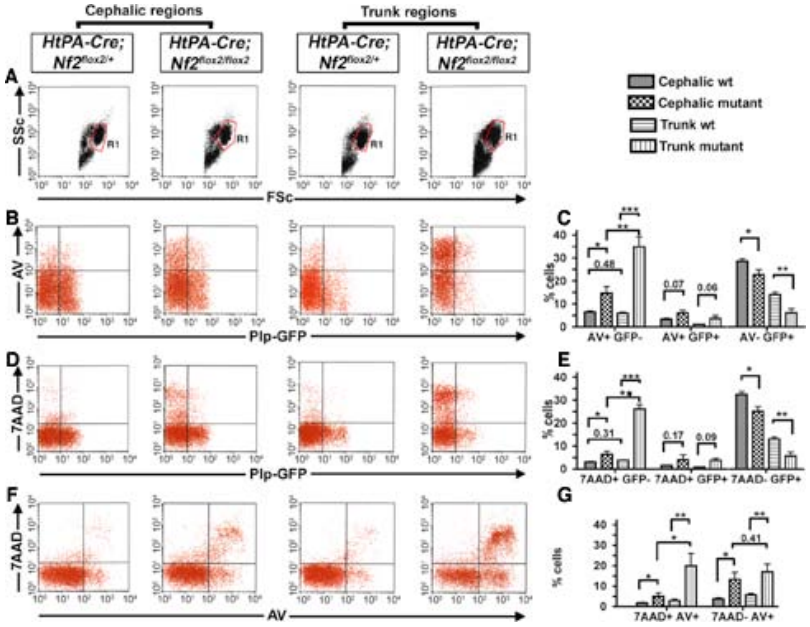

Figure 19. Apoptosis in the cephalic and trunk regions of HtPA-Cre;Nf2$^{flox2/flox2}$ embryos. *At E9.5, cephalic and trunk regions were dissected form Plp-GFP;HtPA-Cre;Nf2$^{flox2/+}$ and Plp-GFP;HtPA-Cre;Nf2$^{flox2/flox2}$ embryos. After digestion, cell suspensions were labelled with the apoptotic markers Annexin V and 7-AAD. FACS analysis showed a stronger increase of apoptotic cells in the trunk region of HtPA-Cre;Nf2$^{flox2/flox2}$embryos. (A) The flow-cytometer was set up to analyze cells plotted in the Region 1 (R1). (B,C) Embryonic cells were analysed for their capacity to label Annexin V and express the Plp-GFP transgene. (B) In each plot, the top right quadrant designs the putative NC cell in apoptosis and the top left quadrant designs GFP negative cells in apoptosis. (D-E) The capacity of embryonic cells to intercalate 7-ADD in their DNA is used to discriminate cells in late stages of apoptosis. (D) In each plot, the top right and top left quadrants design respectively the putative PlpGFP NC cells and the GFP negative cells that were in advanced apoptosis. (F-G) Early apoptotic cells, which are AV+/7AAD-, showed an almost identical percentage in the different regions analyzed. (F) In each plot, the top right and the low right represent respectively the apoptotic cells that were in late and early apoptosis. Asterisks indicate the degree of significance between samples under analysis: Θ = p<0.05, ΘΘ = p<0.01, ΘΘΘ = p<0.001.*

possible that apoptosis is induced indirectly due to the failure of neural tube fusion. Indeed, several targeted mutant mouse strains exhibit both neural tube defaults and altered apoptosis levels. For instance, embryos lacking genes not playing a direct role in apoptosis, such as *ApoB*, *Bcl10*, *Mdm4*, or *Tulp3*, were all associated with increased rates of apoptosis at the edges of improperly closed neural tubes, leading to exencephaly. Besides apoptosis at the open edges of the neural tube, *HtPA-Cre*;*Nf2*$^{flox2/flox}$ mutant embryos showed activated apoptotic programs in the post-migratory NC cell cultures of neural tubes explants *in vitro,* and *in vivo* in the trunk mesenchyme (**Fig. 18H**), supporting the causality of *Nf2* loss in apoptosis induction. Moreover, a broader apoptotic activity was found in the trunk region that appeared more advanced than in the cephalic region, as supported by the lower percentage of 7AAD+/AV+ cells in the cephalic region (**Fig. 19G**). These data, strong reduction of GFP+ NC cells in the trunk region (**Fig. 20**), suggest a scenario where apoptosis begun in the trunk within the *Nf2*$^{-/-}$ NC cells inducing apoptosis of neighboring cells, and leading to death of *HtPA-Cre*;*Nf2*$^{flox2/flox2}$ embryos.

Nf2 Allows Cranial Neural Crest to Coordinate Neural Tube Closure. Neural tube closure is a complex morphogenic process where the neural plate rolls into a tube forming the central nervous system. Cranial neural tube closure is critically dependent on the proliferation and cellular rearrangement of the head mesenchyme. Mice with mutations in genes patterning NC development, such as *Twist1*, *AP-2a*, *Cart1*, and *Nf1*, exhibit cranial neural tube closure defects. *Twist1* and *Cart1* functions are required in the head mesenchyme, where they are expressed in both the paraxial mesoderm and the NC lineages. Deletion of *AP-2a* specifically in the neural crest resulted in exencephaly, indicating that neural crests were essential for cranial neural tube closure. *Nf1*, a gene required for the development of NC-derived structures and the central nervous system, acts as a modifier of folate-sensitive neural tube defects in *Splotch* mice that develop spina bifida and exencephaly (41). Data from the the Giovannini lab enhance our knowledge on the molecular mechanisms leading to cranial neural tube closure, demostrating that *Nf2* is specifically required in NC for normal neural tube development. Finally, these data strongly suggest that a putative deficit of paracrine factors secreted by *Nf2*$^{-/-}$ NC cells could be responsible the neural tube closure defects. Along this line, it has been shown that secretion of FGF8 from NC plays a pivotal role in the neural tube closure of avian embryos (42), indicating a new avenue of research for investigating the molecular mechanisms involving the *Nf2* gene in development and tumorigenesis.

Loss of *Nf2* function in Schwann cells Induces Dedifferentiation and Activation of Nerve Repair Mechanisms by Mimicking Impaired Axon-Schwann Cell Interaction. To understand schwannoma pathophysiology and *NF2* gene function in Schwann cells (SCs), the Giovannini lab compared the transcriptomes of *Nf2*-deficient primary mouse SCs and tumors from *Nf2* mice and NF2 patients. They found that loss of *Nf2* in mouse SCs leads to the activation of a molecular program reminiscent of myelination via the PI3 kinase/Akt pathway. Moreover, primary mouse *Nf2* SC cultures are enriched for genes activated in normal developing immature SCs, supporting tumor dedifferentiation, and mouse schwannoma transcription profiles share striking similarity to developing immature SCs. Comparison of mouse and human schwannoma gene expression lead them to the identification of a common transcriptional signature. Genetic network analysis again revealed significant associations with nerve development and nerve repair wound healing that are normally induced when the axon-SC interaction is disrupted. Altogether, these data suggest that loss of *NF2* mimics loss of axonal contact, thereby inducing

activation of gene programs involved in nerve repair in a cell-autonomous manner. In conclusion, merlin plays a role in axon-SC cross-talk and that loss of this specific function is relevant to schwannoma formation. This provides a novel view on schwannoma development whereby NF2 tumors arise as a consequence of abnormal activation of nerve repair processes in SC that are usually triggered following nerve injury. These new results suggest that inhibition of the molecular program of nerve repair may represent a novel therapeutic approach to control schwannoma growth.

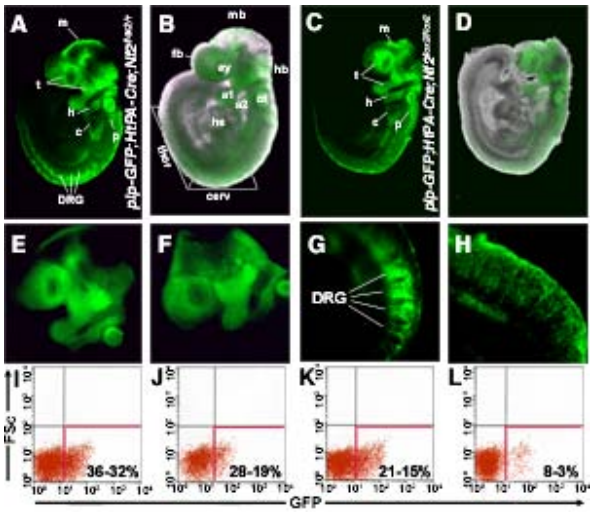

Figure 20. Reduction of Plp-GFP-NC cells in HtPA-Cre;Nf2$^{flox2/flox2}$ embryos *(A-B) At E9.5, Plp-GFP;HtPA-Cre;Nf2$^{flox2/+}$ and Plp-GFP;HtPA-Cre;Nf2$^{flox2/flox2}$ embryos expressed the green fluorescent protein (GFP) in migrating NC. (A) The meningeal (m), trigeminal (t), hyoid (h), cardiac (c) and post-otic NC streams were positive to the GFP. In the trunk, the plp-GFP transgene was expressed in the DRG. (B) Merging of the GFP+ regions and phase contrast embryo images showed that the plp-GFP transgene was expressed in the embryos districts classically described as being colonised by NC cells. The trigeminal stream migrated in the forebrain (fb) and first branchial arch (a1), avoiding the lens placode (ey), and NC cells that will give rise to meninges populated the midbrain regions (mb). From the hindbrain (hb) the hyoid stream surrounded the otic vesicle (ot) and migrated in the second branchial arch (a2). In the hindbrain otic region, the post-otic stream migrated in the most posterior branchial arches and the cardiac stream populated the heart (he). In the trunk the cervical (cerv) and thoracic (thor) somites were populated from those NC cells which lead to DRG formation. (C) plp-GFP;HtPA-Cre;Nf2$^{flox2/flox2}$ embryos showed a strong reduction of GFP expression in the trunk, while their cephalic regions presented the same distribution of GFP+ cells as control embryos. In the cephalic region the trigeminal, the hyoid and the post-otic stream were still well detected, as well as the cardiac flow. The meningeal stream could be only guessed due to failure of neural tube closure. In the trunk, NC cells were scattered and did not form the DRG structures. (D) Merge of the GFP pattern and phase contrast images of a HtPA-Cre;Nf2$^{flox2/flox2}$ embryo. (E, G) High magnification of plp-GFP expression within cephalic and trunk regions of control embryos. (F, H) High magnification of plp-GFP expression within cephalic and trunk regions of mutant embryos. (I-L) FACS plots from cephalic and trunk region of control and mutant plp-GFP embryonic cell suspensions. Each plot represents the cell distribution in function of fluorescence intensity, X-axes, and cell size by forward scatters (FSc), Y-axes. In the low-right quadrants are NC cells expressing the Plp-GFP transgene, the lower and higher percentage of GFP positive cells over 3 repeats is indicated in the quadrant. (I,K) The pre-otic cephalic regions dissected from wild type and mutant plp-GFP embryos showed no significant differences in the ratio of GFP+ cells. (O,P) The post-otic trunk region dissected from wild type and mutant plp-GFP embryos showed a strong reduction of GFP+ cells in the mutant embryos.*

<u>*Nf2* in Wound Healing: Injury as a Mechanism of Tumor Initiation</u>. Injury is required for adeno-Cre administration to the meninges of adult mice; therefore, it was not possible to distinguish the relative roles of injury and somatic genetic changes in meningioma initiation. To address the potential role of injury directly and to determine whether *Nf2* loss and *Kras* activation would result in other tumor types associated with NF2, the Jacks lab developed a tumor model in the sciatic nerve, which is readily accessible to manipulation in the posterior thigh. Because adeno-Cre was not able to penetrate intact sciatic nerve (data not shown), mice were bred onto the *R26-CreER^{T2}* strain. In the sham operated nerves, they found that *NF2* deletion resulted in increased cellularity compared to control nerves as evidenced by an increase in density of Schwann cell nuclei (low grade hyperplasia or LGH). *Kras* activation also resulted predominantly in LGH in sham operated nerves. The combination of *Nf2* loss and *Kras* activation resulted in nearly 40% of sham operated nerves with tumor formation, suggesting synergism between a proliferative *Kras* stimulus and disruption of the ability to form normal cell-cell junctions by *Nf2* loss.

To evaluate the role of injury in tumor formation, nerves were transected in the proximal 1/3 of the thigh and a 3 mm segment was removed to inhibit regrowth. In 23% of control nerves, this resulted in formation of traumatic neuromas, a non-neoplastic mass of disorganized axons and Schwann cells that can form when severed nerves are unable to locate and re-innervate their targets. It was not possible to distinguish traumatic neuromas (TNs) from potential low grade tumors (LGTs) by histology; therefore, they were grouped into a single grade for analysis (LGT/TN). This was part of a tumor grading system developed in collaboration with a veterinary pathologist in light of recent guidelines for analysis of genetically-engineered mouse models of neurofibromatosis. Of *Nf2;CreER* injured nerves, 33% demonstrated LGT/TN pathology. By contrast, *K;CreER* injured nerves demonstrated LGT/TN or medium grade tumor (MGT) formation in 18/21 mice. In *K;Nf2;CreER* mice, 100% (11/11) of injured nerves formed tumors.

To further investigate the course of tumor progression in the setting of *K-ras*^{G12D} activation, a cohort of *K;Nf2* and control mice were administered adeno-Cre to injured nerves. Due to this more localized method of Cre delivery, mice did not develop papillomas or other systemic effects. At approximately 6 months post-injury, the *K;Nf2* mice developed large, 2-3 cm tumors at the injured nerve site that contained scattered S100 staining and tumor metastasis to the lung (**Figure 21**). These findings are consistent with transformation of a Schwann cell derived tumor to a malignant peripheral nerve sheath tumor (MPNSTs).

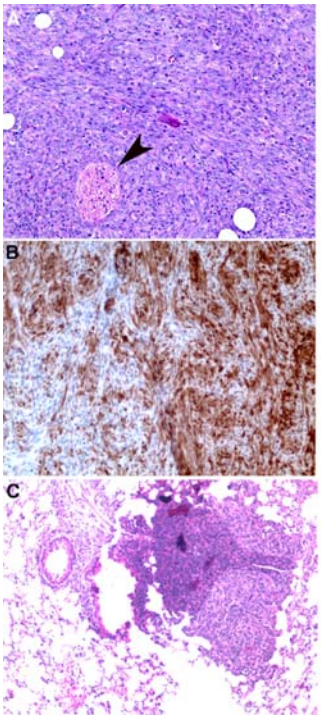

Figure 21. K;Nf2;CreER nerve tumors undergo malignant transformation
To avoid effects of systemic activation of K-ras^{G12D} *in the schwannoma/PNST model with the R26-CreER*^{T2} *allele, adeno-Cre was administered to the injured sciatic nerves of K;Nf2 mice. These nerves enlarged to form tumors approximately 2 cm in size over a period of 6 months, demonstrated a high grade histopathology with frequent mitoses and high nuclear to cytoplastic ratio (A), were locally invasive, and metastasized to the lung (C). These tumors retained S100 staining consistent with Schwann cell origin (B). Arrowhead in A indicates a normal nerve fascicle trapped within the tumor. Panels A and B were taken at original magnification of 200X and C at 100X.*

Adult Onset Tumors in an NF1 Mouse Model Also Requires Injury**.** Rosa26-CreER^{T2}; *Nf1*$^{flox/-}$ mice (which are effectively heterozygous *Nf1* mutant) were used to study the effect of *Nf1* loss in sporadic cells following tamoxifen administration. Neurofibromas were induced at different stages of development by administering tamoxifen either systemically or through the skin by dissolving in DMSO. After 4-6 months, mice did not develop any gross dermal neurofibromas. Surprisingly, the Jacks Lab identified a key role of injury in the induction of neurofibromas in peripheral nerve (**Figure 22A-F**). Ras is activated in Schwann cells following injury to initiate the cell de-differentiation and proliferation required for nerve repair. Loss of neurofibromin may impair Ras regulation during the repair process and thereby lead to dysregulated Schwann cell proliferation and tumor formation. By contrast, dermal neurofibromas never occurred in adult skin with or without injury when mice were aged as long as 1 year following *Nf1* deletion. However, when combined with deletion of the *p16*^{Ink4a}/*p19*^{Arf} locus, large neurofibromas developed within 2-3 months in 70% of treated mice (Figure 22G-I). These results demonstrate that senescence pathways restrict neurofibroma formation in adult skin but not nerve. Together, these results yield insight into tissue specific mechanisms underlying transformation of mature cells in a mouse model of NF1.

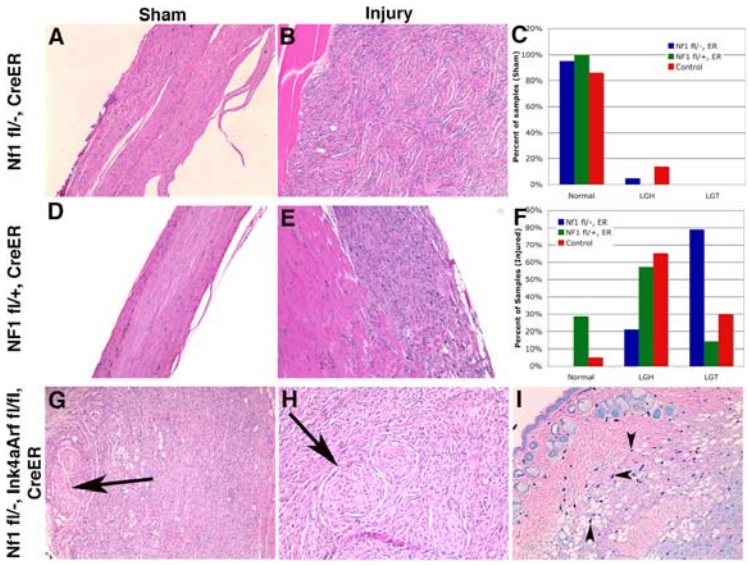

Figure 22. Modeling adult onset tumors in NF1. *Adult Nf1*$^{fl/-}$*;R26-CreER*^{T2} *(A, B) or Nf1*$^{fl/+}$*;R26-CreER*^{T2} *(D, E) mice underwent sham operation (A,D) or injury (B, E) of their sciatic nerves. The floxed NF1 allele was deleted by local 4-hydroxy-tamoxifen administration at the time of surgery. No significant change in nerve histology was observed following NF1 deletion and sham operation compared to control nerves (C); but with injury, NF1 loss resulted in low grade tumor formation in 80% of treated nerves (F). Neurofibromas formed in the dermis following NF1 deletion in adult cells when combined with deletion of the p16*^{Ink4a}*/p19*^{Arf} *tumor suppressor locus (G, H, I), but not with NF1 deletion alone. These tumors showed a strong mast cell infiltrate (arrowheads, I), similar to human dermal neurofibromas. All images taken with the 10X lens except H (20X) and were stained with hematoxylin and eosin except I (Wright-Giemsa). LGH=low grade hyperplasia, LGT=low grade tumor. Arrows (G,H) indicate nerves trapped within the neurofibromas.*

Differential Effects of a MEK Inhibitor in *Mx1-Cre, Nf1*$^{flox/flox}$ Mice with MPD and AML. The Shannon lab recently administered MEK inhibitors to *Mx1-Cre, Nf1*$^{flox/flox}$ mutant mice that developed a JMML-like MPD due to *Nf1* inactivation in bone marrow cells with a second cohort in which they used retroviral insertional mutagensis to induce mutations that cooperate with loss of *Nf1* and produce acute myeloid leukemia (AML)(43). *Nf1* inactivation was associated with a higher incidence of AML in mice that received the MOL4070 retrovirus, and these leukemia developed with reduced latency (data not shown). *Mx1-Cre, Nf1*$^{flox/flox}$ mice predominately developed invasive AML with myeloblasts in blood and marrow, extensive tissue infiltration, and myeloid markers detected by flow cytometry. The Shannon obtained CI-1040 from Pfizer, Inc., and found that 25-50 µM of CI-1040 abrogated colony forming unit

granulocyte macrophage (CFU-GM) colony formation from *Mx1-Cre, Nf1$^{flox/flox}$* bone marrow in response to GM-CSF. Importantly, however, there was no therapeutic index as CFU-GM growth from wild-type (WT) bone marrow was inhibited at similar concentrations (**Fig. 23A**). The Shannon lab next established 100 mg/kg administered twice a day as the maximally tolerated dose (MTD) of CI-1040 in WT mice, and measured inhibition of pERK induction by GM-CSF at this dose. This pharmacodynamic (PD) analysis revealed profound MEK inhibition 2 hours following CI-1040 administration, with inhibition of ~50% after 4 hours and no detectable effect at 8 hours (data not shown). *Mx1-Cre, Nf1$^{flox/flox}$* mice with MPD (n=10) that were randomized to 28 days of treatment with CI-1040 showed no improvement in leukocyte counts or splenomegaly (data not shown).

By contrast, blast colony growth from *Mx1-Cre Nf1 $^{flox/flox}$* AML bone marrow was abrogated at much lower drug concentrations of CI-1040 (**Fig. 23A**). These unexpected data suggested that mutations that are acquired during progression from MPD to AML render leukemic cells that have inactivated *Nf1* more dependent on Raf/MEK/ERK signaling. To test this hypothesis, the Shannon performed a second trial in 25 recipient mice that were transplanted with 4 independent leukemias. These mice were randomized to treatment with either CI-1040 or control vehicle at the MTD, which had no beneficial effect in mice with MPD. The MEK inhibitor had dramatic effects in this setting. Whereas the leukocyte counts of vehicle-treated mice increased progressively, these counts declined in mice that were randomized to receive CI-1040 (**Fig. 23B**). Treatment with CI-1040 was also associated with markedly prolonged survival (24 versus 7 days in the vehicle-treated cohort; odds ratio 3.5, 95% CI 3.0-3.8) (**Fig. 23C**). These data infer that the therapeutic response to a molecularly-targeted inhibitor is strongly modulated by the genetic context in which a disease-initiating mutation occurs. Specifically, while there was no beneficial therapeutic index in *Nf1* mutant mice with MPD that were treated with CI-1040, progression to AML was associated with enhanced sensitivity to this agent.

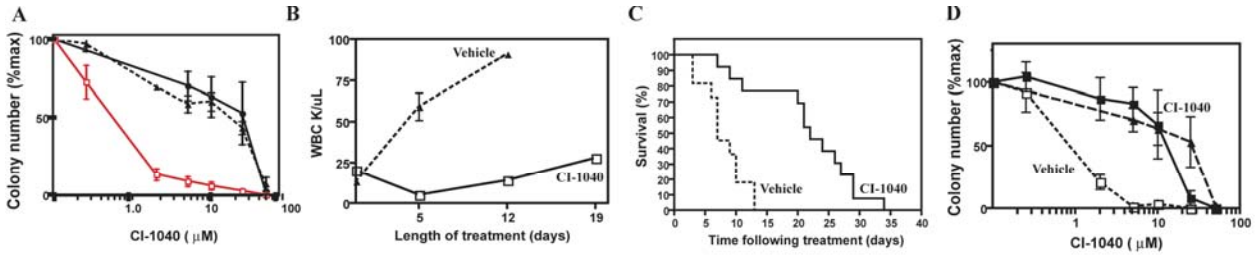

Figure 23. Response and resistance to CI-1040 in Mx1-Cre, Nf1$^{flox/flox}$ mice with AML. ***(A)*** *Myeloid colony growth from the marrows of WT mice (circles, n=12), Mx1-Cre, Nf1$^{flox/flox}$ mice with MPD (triangles, n=6) and AML (squares, n=8) over a range of CI-1040 concentrations (log scale).* ***(B)*** *Leukocyte counts were markedly decreased in mice treated with CI-1040 (n=13) compared to the vehicle (n=12).* ***(C)*** *Survival was prolonged three-fold in mice that received CI-1040 (OR 3.1; CI 2.7-3.6; p < 0.0001).* ***(D)*** *Myeloid colony growth from the bone marrows of mice with recurrent leukemia are less sensitive to CI-1040 inhibition than the parental AMLs. Colony growth in methylcellulose is shown for WT bone marrow (closed squares, n=2), for a primary AML that was harvested from a vehicle-treated mouse (open squares, n=4), and from a mouse that was transplanted with the same AML that responded initially to CI-1040 but relapsed (closed triangles, n=3). Error bars represent SEM.*

Resistance to MEK Inhibitors Is Due to Outgrowth of Preexisitng Clones. CI-1040-treated mice eventually relapsed and died of AML despite continued treatment. These leukemias were remarkably less sensitive to CI-1040 *in vitro* than the parental AMLs (**Fig. 23D**), and did not respond to CI-1040 in secondary recipients. The Shannon lab observed equivalent inhibition of pERK in sensitive and resistant AMLs that were exposed to CI-1040, which indicate that resistance is not due to acquired *MEK1* mutations that render the kinase insensitive to the drug (data not shown). To address if *de novo* resistance is associated with genetic evolution of the leukemic clone, performed Southern blot analysis was performed with a MOL4070LTR-specific probe. Analysis of sensitive/resistant pairs revealed novel restriction fragments in the resistant leukemias that we isolated from multiple independent recipient mice (**Fig. 24A**). This observation provided compelling evidence that the resistant clone is present at undetectable levels in the primary AML. To identify candidate genes that might influence response to CI-1040, we exploited a shotgun cloning strategy that provides information regarding both the identity and frequency of proviral integrations (44) to comprehensively characterize mutations in two sensitive and resistant leukemia pairs. The functional analysis of one of these leukemias (AML #6537) is presented below.

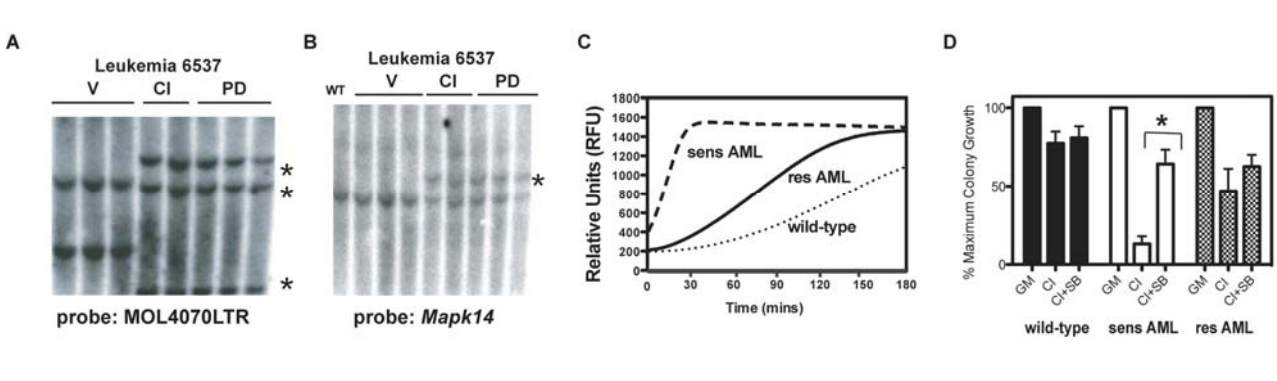

Figure 24*. Characteristics of sensitive and resistant AMLs. (A)** *Retroviral integrations in DNA samples from AML #6537 in independent mice following treatment with Vehicle (V), CI-1040 (CI) or the second generation MEK inhibitor PD0325901 (PD). Asterisks denote restriction fragments that are only present in resistant AMLs.* ***(B) *Southern blot analysis of sensitive and resistant leukemias with a Mapk14 probe. The resistant leukemias shown in lanes CI and PD show a new Mapk14 hybridization fragment, which overlaps with one of the MOL4070LTR bands in the resistant leukemias shown in panel A. Note that a fragment corresponding to the normal Mapk14 allele is present in the resistant leukemia, and is reduced in intensity.* ***(C)*** *Basal p38 kinase activity of resistant AML #6537 cells (solid line) is reduced in comparison to the parental leukemia (heavy dashed line). All leukemias demonstrate elevation of p38 kinase activity over WT marrow (dotted line).* ***(E)*** *The p38a inhibitor, SB202190 (SB), antagonizes the ability of CI-1040 (CI) to inhibit blast colony inhibition in parental AML #6537. CI-1040 (2.5 mM) has a modest inhibitory effect on WT CFU-GM colony growth, which is not affected by 2.5 mM SB202190 (solid black bars, n=8). SB rescues the ability of sensitive AML #6537 to form blast colonies under these conditions (solid white bars, n=7). By contrast, blast colony growth in resistant AML #6537 (checkered bars, n=5) is less sensitive to CI-1040 and is unaffected by the addition of SB. Error bars represent the SEM. AML blast colony growth of sensitive AML #6537 is significantly increased by the addition of SB to CI-1040 (p= 0.0043; unpaired t-test).*

As expected from the Southern blot data (**Fig. 24A**), novel retroviral integrations were identified in resistant AML #6537 that were not recovered from the sensitive parental leukemia. A major integration site in this resistant AML is within *Mapk14*, which encodes p38α. Quantitative RT-PCR of proviral/host DNA junctions confirmed that the inserted allele copy

number is increased 1,000 fold (range 1,000-10,000 fold) in the resistant leukemias. The proviral insertion is in the anti-sense orientation and Southern blot analysis supports inactivation of one *Mapk14* allele (**Fig. 24B**). Consistent with this prediction, basal p38α kinase activity is reduced in resistant AML #6537 relative to the sensitive leukemia (**Fig. 24C**). To further investigate if decreased p38α activity modulates resistance to MEK inhibitors in primary leukemia cells, the Shannon lab enumerated blast colonies from AML #6537 in methylcellulose cultures containing CI-1040, SB202190 (a specific inhibitor of p38α)) or both drugs. SB202190 strongly antagonized the inhibitory effects of CI-1040 on the sensitive leukemia, but had minimal effects on the resistant AML (**Fig. 24D**). These data further supports the hypothesis that *Mapk14* haploinsufficiency contributes to resistance. In depth analysis of a second sensitive/resistant pair (AML #6554) demonstrated over-expression of *Rasgrp1,* which encodes a guanine nucleotide exchange factor for Ras, modulates MEK resistance *in vivo.* Together, these studies provide "proof of principle" that treating primary cancers with targeted agents *in vivo* followed by the subsequent genetic and functional analysis of paired sensitive and resistant clones is a potent and unbiased strategy for uncovering genes that underlie "off target" resistance to molecular therapeutics. These efforts are greatly facilitated by the use of insertional mutagenesis strategies, which insert a sequence tag that can be used to interrogate clonal progression and to isolate candidate resistance genes.

KEY RESEARCH ACCOMPLISHMENTS

(a) The investigators have extensively shared expertise and reagents to pursue common research goals throughout the duration of this award.

(b) We found that the loss of contact-dependent inhibition of proliferation exhibited by *Nf2*-deficient Schwann cells, is Nrg-dependent, associated with increased ErbB2:3 heterodimerization and dependent on both ErbB3 and the PDZ-domain containing adapter NHE-RF1. We also found that NHE-RF1 associates with Merlin and ErbB3 and is central to Merlin-mediated regulation of ErbB3 signaling in SCs.

(c) We found that the subcutaneous growth of $Nf2^{-/-}$ SCs or establishment of SC lines in the absence of the SC mitogen neuregulin leads to upregulation and activation of EGFR and downregulation of ErbB3.

(d) We have found that alterations in the levels of and signaling from ErbB receptors occurs in several types of *Nf2*-deficient epithelial tissues and that inhibition of ErbB signaling can halt the overproliferation of $Nf2^{-/-}$ cells in vitro and lesions in mice *in vivo*.

(e) We have generated a strain of mice carrying a conditional inactivating mutation in the gene encoding Expanded, a physical and genetic interactor of Nf2/Merlin in the fruitfly.

(f) We have refined our mouse models of neurofibromas through the isolation of precursor cells that can be genetically manipulated and introduced into the same mouse to form tumors.

(g) MPNST-derived cells are being tested to discover novel molecules that may interrupt their growth in collaboration with the chemical screening facility at UTSW Department of Biochemistry.

(h) We have developed a robust model for NF1-associated optic glioma. These mice are now being placed in preclinical trials for prevention and tumor arrest therapies.

(i) We have developed a robust model for NF1-associated astrocytoma. We have identified the cells that give rise to the tumor, purified them, and are in the process of screening for chemical compounds that inhibit growth.

(j) We have developed a robust model for dermal neurofibromas that completely replicate the human tumors. These mice will serve as substrates for preclinical testing.

(k) Studies performed in mouse neurofibroma led directly to a phase II clinical trials using imanitib to treat plexiform neurofibromas. The rationale for this novel trial is based on the ability to regress plexiform neurofibromas in our mice by inhibiting mast cell function.

(l) A new method was developed for isolating mitotically active SCs that can also be used for the purification/enrichment of early NCC-derived cells.

(m) A novel strain of drug-inducible Cre mice was constructed and has been harnessed to develop models of adult onset tumors by deleting the Nf1 and Nf2 genes in specific tissues at defined time points.

(n) A role for injury in tumor initiation was demonstrated in both NF1 and NF2 mouse models.

(o) Synergy between Ras activation and merlin loss enabled us to model nearly all tumor types frequently seen in NF2 patients including cranial nerve schwannomas, meningiomas, PNSTs, MPNSTs and ependymal hyperplasia.

(p) The results of these studies add further impetus to the idea that loss of Ras regulation by merlin may be key to tumor initiation and/or progression in NF2 patients.

(q) Since the Ras-Raf-MEK-signaling pathway has been found to be frequently dysregulated in human tumor samples of these types, mechanisms that underlie interactions between merlin and the Ras-signaling pathway, including Rac and Pak, may serve as key drug targets

(r) A novel strain of drug-inducible Cre mice was constructed and is being harnessed to develop models of adult onset tumors by deleting the *Nf1* and *Nf2* genes in specific tissues at defined time points.

(s) We have begun characterizing the role of *Nf2* in wound healing and the role of injury in tumor initiation.

(t) We have observed cooperative tumorigenic effects of *Nf2*-loss and oncogenic *Kras* expression in a model of ependymona and in schwannoma formation.

(u) Studies of MEFs and bone marrow cells support the idea that p120GAP functions both as a negative regulator of Ras signaling and to promote growth.

(v) The biochemical consequences of *Nf1* inactivation in primary cells was investigated by Western blotting and by phospho-FACS analysis of bone marrow cells from *Mx1-Cre* $Nf1^{flox/flox}$ mice.

(w) RIM was used to generate aggressive leukemias, to identify genes and pathways that cooperate with *Nf1* inactivation in tumorigenesis, and to investigate mechanisms of response and resistance to MEK.

(x) We have developed robust models of radiation-induced cancers in *Nf1* mice that accurately model human clinical protocols and can be used for biologic, preclinical, and chemopreventive studies

(y) We have demonstrated a role for *Nf2* in neural crest patterning and development

(z) We found that loss of *Nf2* in Schwann cells induces dedifferentiation and activation of nerve repair mechanisms.

(aa) We have demonstrated that tumor suppression functions of merlin are independent of its role as an organizer of Schwann cell actin cytoskeleton.

(bb) We demonstrated that merlin regulates transmembrane receptor accumulation and signaling at the plasma membrane of normal and tumoral Schwann cells.

(cc) The strains of *Nf1* and *Nf2* mutant mice developed through this effort have been shared widely with the NF research community (see list below in Reportable Outcomes) and comprise an integral resource of the Preclinical Drug Discovery Initiative of the Children's Tumor Foundation. Through these collaborative experiments, the scientific value of this consortium has extended well beyond the studies being pursued in the participant's laboratories.

REPORTABLE OUTCOMES

(a) Research Articles and Reviews Supported by This Award

2006

Bonilha VL, Rayborn ME, Saotome I, **McClatchey AI,** Hollyfield JG. Microvilli defects in retinas of ezrin knockout mice. *Exp Eye Res.* 2006; **82:** 720-9.

Yang, F., Chen, S, Clegg, T., Li, X., Morgan, T., Estwick, S.A., Yuan, J., Khalaf, W., Burgin, S., Travers, J., **Parada, L.F.,** Ingram, D.A., and Clapp, D. W. Nf1+/- Mast Cells Induce Neurofibroma Like Phenotypes Through Secreted TGFβ Signaling. *Hum Mol Genet.* 2006; **15:** 2421-37.

Elefteriou, F. Benson, M.D., Sowa, H., Starbuck, M., Liu, J., Ro, D., **Parada, LF** and Karsenty, G. ATF4 mediation of *NF1* pathology in bone reveals a nutritional basis for congenital skeletal dysplasias. *Cell Metabolism* 2006; **4**: 441-51

2007

Kim A*, Morgan K*, Hasz DE, Wiesner SM, Lauchle JO, Geurts JL, Diers MD, Le DT, Kogan SC, **Parada LF, Shannon K**, Largaespada DA. β common receptor inactivation attenuates myeloproliferative disease in *Nf1* mutant mice. *Blood* 2007; **109:** 1687-9. * these authors contributed equally.

Kolanczyk, M., Kossler, N., Kuhnisch, J., Lavitas, L., Stricker, S., Wilkening, U., Manjubala, I., Fratzl, P., Sporle, R., Herrmann, B.G., **Parada, L.F.,** Kornak, U. and Mundlos, S. Multiple Roles for neurofibromin in skeletal development and growth." *Human Mol Genet* 2007; **16:** 874-886.

Romero, M.I., Lin, L, Lush, M.E., Lei, L., **Parada, L.F**. and Zhu, Y. Deletion of NF1 in neurons induces increased axon collateral branching after dorsal root injury. J Neuroscience 2007; **27:** 2124-34.

Le, L. and **Parada, L.F.** Tumor Microenvironment and Neurofibromatosis Type I: Connecting the GAPs. Oncogene**.** 2007; **12:** 4609-4616.

McLaughlin, M.E., Kruger, G.M., Slocum, K.L., Crowley, D., Michaud, N.A., Huang, J., Magendantz, M., and **Jacks, T.** The *Nf2* tumor suppressor regulates cell-cell adhesion during tissue fusion. *PNAS* 2007; **104:** 3261-3266.

Kalamarides M, Stemmer-Rachamimov AO, Takahashi M, Han Z-Y, Chareyre F, Niwa-Kawakita M, Black PM, Carroll RS, **Giovannini M.** Natural history of meningioma development in mice reveals a synergy in *Nf2* and *p16*Ink4a mutations. *Brain Pathology* 2008 Jan;18(1):62-70.

Curto M, Cole BK, Lallemand D, Liu CH, **McClatchey AI.** Contact-dependent inhibition of EGFR signaling by Nf2/Merlin. *J Cell Biol*. 2007; **177:** 893-903.

Schubbert S, Bollag G, **Shannon K.** Deregulated Ras signaling in developmental disorders: new tricks for an old dog. *Curr Opin Genes Develop* 2007; **17:** 15-22.

Schubbert S, **Shannon K,** Bollag G. Hyperactive Ras signaling in developmental disorders and cancer. *Nat Reviews Cancer* 2007; **7:** 295-308.

Diaz-Flores, E and **Shannon K**. Targeting oncogenic Ras. *Genes Develop* 2007; **21:** 1989-92.

2008

Curto, M, **McClatchey, AI.** Nf2/Merlin: A coordinator of receptor signaling and intercellular contact. *The British Journal of Cancer*, 2008; **98(2):**256-62.

Cole, B, Curto, M, **McClatchey, AI.** Localization to the cortical cytoskeleton is necessary for Nf2/Merlin-dependent EGFR silencing. *Mol Cell Biol* 2008; **28**:1274-84.

Joseph, N.M., Mosher J.T., Buchstaller J., Snider P., McKeever P.E., Lim M., Conway S.J., **Parada L.F**., Zhu Y. "The loss of Nf1 transiently promotes self-renewal but not tumorigenesis by neural crest stem cells." *Cancer Cell* 2008; **13**: 129-40.

Lush, M. E., Li, Y., Kwon, C.H., Chen, J. and **Parada, L.F.** "Neurofibromin is required for barrel formation in the mouse somatosensory cortex." *Journal of Neuroscience* 2008; **28(7)**: 1580-87.

Kwon, C.H., Zhao, D., Chen, J., Alcantara, S., Li, Y., Burns, D., Mason, R., Lee, E. Y-H., Wu, H. and **Parada, L.F.** Pten Haploinsufficiency Accelerates Formation of High Grade Astrocytomas." *Cancer Research* 2008; **68(9)**: 3286-94.

Yang, F.C., Ingram, D.A., Chen, S., Zhu, Y., Yuan, J., Li, X., Yang, X, Knowles, S., Horn, W., Li, Y., Zhang, S., Yang, Y., Vakili, S., Yu, M., Burns, D., Robertson, K., Hutchins, G., **Parada, L.F.*,** and Clapp, D.W. *NF1*-dependent tumors require a microenvironment containing *Nf1+/-* and c-kit dependent bone marrow." *Cell* 2008; **135:** 437-448. (* co-corresponding author)

Cui, Y., Costa, R.M., Murphy, G.G., Elgersma, Y., Zhu, Y., Gutmann, D.H., **Parada, L.F**., Mody, I., and Silva, A. "Neurofibromin regulation of ERK signaling modulates GABA release and learning." *Cell* 2008; **135(3)**: 549-60.

Farassati, F., Pan, W., Yamoutour, F., Henke, S., Piedra, M., Frahm, S., Al-Tawil, S., Mangrum, W.I., **Parada, L.F.**, Rabkin, S.D., Martuza, R.L. and Kurtz, A. "Ras signaling influences permissiveness of malignant peripheral nerve sheath tumor cells to oncolytic herpes." *American Journal of Pathology* 2008; **173(6)**: 1861-72.

Alcantara Llaguno, S., Chen, J., Kwon, C.-H., and **Parada, L.F.** "Neural and cancer stem cells in tumor suppressor mouse models of malignant astrocytoma." *Cold Spring Harbor Symposia on Quantitative Biology* 2008; **73**: 421-26.

Parrinello, S., Noon, L.A., Harrisingh, M.C., Digby, P.W., Rosenberg, L.H., Cremona, C.A., Echave, P., Flanagan, A.M., **Parada, L.F**., and Lloyd, A.C. "NF1 loss disrupts Schwann cell-axonal interactions: a novel role for semaphorin 4F". *Genes & Development* 2008; **22(23)**: 3335-48.

2009

Lauchle JO, Kim D, Le DT, Akagi K, Gorman M, Krisman K, Crone M, Bonifas JM, Li Q, Tran M, Przybranowski S, Diaz-Flores E, Peterson A, Knab B, Kogan SC, Roose J, Copeland N, Jenkins N, **Parada LF,** Wolff L, Leopold J, **Shannon K.** Response and resistance to MEK inhibition in leukemias initiated by hyperactive Ras. *Nature* 2009; *461*, 411-414.

Yin B, Delwel R, Valk PJ, Wallace MR, Loh ML, **Shannon KM**, Largaespada DA. A retroviral mutagenesis screen reveals strong cooperation between Bcl11a overexpression and loss of the *Nf1* tumor suppressor gene. *Blood* 2009; **113:**1075-85.

Morris, ZS, **McClatchey, AI**. Aberrant epithelial morphology and persistent EGFR signaling in a mouse model of renal cell carcinoma. *Proc Nat Acad Sci,* 2009; **106(24):**976-82.

McClatchey, AI, Fehon, RG. Merlin and the ERM proteins – regulators of membrane distribution and signaling at the cell cortex. *Trends in Cell Biology*, 2009; **19(5):**198-206.

Morris, ZS, **McClatchey, AI.** The neurofibroma cell of origin: SKPs expand the playing field. *Cell Stem Cell* 2009; **4(5)**:371-2.

Alcantara Llaguno, S., Chen, J., Kwon, C.H., Jackson, E.L., Li, Y., Burns, D.K., Alvarez-Buylla, A., and **Parada, L.F**. "Malignant astrocytomas originate from neural stem/progenitor cells in a somatic tumor suppressor mouse model". *Cancer Cell* 2009; **15(1):** 45-56.

Le, L., Shipman, T., Burns, D.K., and **Parada, L.F.** "Cell of origin and microenvironment contribution for NF1-associated dermal neurofibromas." *Cell Stem Cell* 2009; **4(5):** 453-63.

Bodempudi, V., Yamoutpoor, F., Pan, W., Dudek, A.Z., Esfandyari, T., Piedra, M., Babovick, D., Woo, R.A., Mautner, V.F., Kluwe, L., Clapp, D.W., Devries, G.H., Thomas, S.L., Kurtz, A., **Parada, L.F.**, and Farassati, F. "RAL overactivation in malignant peripheral nerve sheath tumors." *Molecular Cell Biol.* 2009; **Jul;29(14):** 3964-74. Epub 2009 May 4.

Lin, L., Chen, J., Richardson, J.A., and **Parada, L.F.** "Mice lacking neurofibromin develop gastric hyperplasia." *Am J Physiol Gastrointest Liver Physiol.* 2009; **Aug 6.**

Lallemand D, Manent J, Couvelard A, Watilliaux A, Siena M, Chareyre F, Lampin A, Niwa-Kawakita M, Kalamarides M, and Giovannini M. "Merlin regulates transmembrane receptor accumulation and signaling at the plasma membrane in primary mouse Schwann cells and in human schwannomas." *Oncogene. 2009* **Feb 12;28(6):**854-65.

Submitted or in Press

Curto, M, Saotome I, McClatchey, AI. Tumorigenic expansion of liver stem/progenitor cells after loss of *Nf2*/Merlin. (*in revision*).

Morris, ZS, Baca, Q, Curto, M, Golan, DE, McClatchey, AI. NF2/Merlin controls lateral mobility, membrane distribution and internalization of EGFR. (*in revision*).

Fehon, RG, McClatchey, AI, Bretscher, A. Organizing the cell cortex: The role of ERM proteins. *Nature Rev Cell Mol Biol* (*invited and under peer review*).

Gladden, AB, Hebert, AM, Schneeberger, A, McClatchey AI. The NF2 tumor suppressor, Merlin, regulates epidermal development through the establishment of a junctional polarity complex. (*submitted*).

Kruger GM, Magendantz M, Sinha I, Chaber CJ, Crowley D, Bronson R, McLaughlin ME, and Jacks T. Loss of *Nf2* synergizes with oncogene activation and tissue injury in mice to recapitulate the adult onset tumors typical of neurofibromatosis type II patients. *Cancer Research*, under review.

Alcantara Llaguno, S.R., Chen, J., and **Parada, L.F.** "Signaling in malignant astrocytomas: role of neural stem calls and its therapeutic implications."In press.

Manent J, Jessen WJ, Niwa-Kawakita M, Kalamarides M, Kaiser S, Ratner N, Aronow BJ, and Giovannini M. Loss of *NF2* function in Schwann cells induces dedifferentiation and activation of nerve repair mechanisms by mimicking impaired axon-Schwann cell interaction. *Submitted.*

Martinelli C, Watilliaux A, Büchmann-Møller S, Dufour S, Sommer L, and Giovannini M. *Nf2* loss in mouse neural crest causes neural tube defaults and early embryonic lethality by inducing massive apoptosis. *Submitted.*

Lallemand D, Lampin A, and Giovannini M. Tumor suppression functions of merlin are independent of its role as an organizer of Schwann cell actin cytoskeleton. *Journal of Cell Science,* In press.

(b) Model Development and Distribution to the Research Community

Studies conducted to date have established a number of novel models of NF1 and NF2-associated tumors and have generated several new strains of mice. *Nf1* and *Nf2* mutant mice have been deposited in the MMHCC Repository where they are readily available to the research community. In addition, the participants in this Consortium have provided strains directly to the investigators listed below. In addition, for purposes of safekeeping and efficiency, the Jacks Lab have deposited all their mouse strains at the Jackson Laboratories in Maine (clean barrier), including

Nf2+/- mice
http://jaxmice.jax.org/strain/008190.html

Nf1+/-p53+/-CIS
http://jaxmice.jax.org/strain/008191.html

Nf1+/-
http://jaxmice.jax.org/strain/008192.html

ROSA-CreER
http://jaxmice.jax.org/strain/008463.html

The research community will thus have continued access to these mice upon completion of this grant.

Karlene Reilly (National Cancer Institute)
Jeffrey DeClue (National Cancer Institute)
Jonathan Epstein (University of Pennsylvania)
D. Wade Clapp (Indiana University)
David Guttmann (Washington University)
David Largaespada (University of Minnesota)
Jeffrey Lawrence (UCSF)

Alcino Silva (UCLA)
Gerard Karsenty (Baylor)
Shaojun Tang (UC Irvine)
Shalom Avraham (Beth Israel)
James Bieker (Mount Sinai, New York)
Abhijit Guha (Labatt Brain Tumor Research Center, Tornoto)
Andreas Kurtz, (Harvard)
Jim Gussella (Harvard)
Dan Haber (Harvard)
Antonio Chiocca (Harvard)
Isidro Sanchez-Garcia (IBMCC)
Victor Tybulewicz (National Institute for Medical Research, London)
Lindsay Hinck (UC Santa Cruz)
Keqiang Ye (Emory University School of Medicine)
Lynda Chin (Dana Farber Cancer Institute)
Joseph Testa (Fox Chase Cancer Center)
Nancy Ratner (U. of Cincinnati)
Stefan Mundlos (U. of Berlin)
Juha Peltonen (U. of Helsinki, Finland)
Warren Pear (University of Pennsylvania)
David Beebe (Washington University)
Filippo Giancotti (MSKCC, New York)
Joe Kissil (Wistar Institute, Philadelphia)
Long Sheng Chang (Ohio State University, Columbus)
Cristina Fernandez Valle (University of Central Florida, Orlando)
Silvia Espejel (University of California, San Francisco)
Karen Cichowski, (Harvard)
Sean J. Morrison, (University of Michigan)
John J. Ryan, (Virginia Commonwealth University)
Isa Hussaini, (University of Virginia)
William Pu, (Children's Hospital, Boston)
Filippo G. Giancotti (Sloan-Kettering Institute for Cancer Research)
David Wilkes (Cornell University Medical College)
Ivan Radovanovic (Geneva)
Brian Weiss (University of Cincinnati)
Arturo Alvarez-Buylla (University of California, San Francisco)
Jonathan Chernoff, (Fox Chase Cancer Center)
Laurent Elefteriou (UT San Antonio)
David Kaplan (Toronto)
Hong Wu (UCLA)
Ugur Ozerdem (La Jolla Insitiute)
David Ingram (Indiana U)
Takayuki Harada (Tokyo)
Alison Lloyd (London, UK)
Junichi Sadoshima (New Jersey Medical School and Johns Hopkins)
Susan Lindquist (Whitehead Institute at MIT)

Richard Bram (Mayo Clinic Rochester)
Jean Nakamura (University of California, San Francisco)
Kevin Haigis (MGH)
David Scadden (MGH)
Neetu Gupta (Cleveland Clinic)
Fred Gage (Salk Institute)
David Parkinson (Peninsula Medical Center)
Kathryn Yamada (Washington University)
Fernando Camargo (MIT)
Mario Capecchi (University of Utah)
Marlan Hansen (University of Iowa)
Helen McNeill (Mount Sinai Hospital, Toronto)
Rakesh Jain (MGH)
Duojia Pan (Johns Hopkins University School of Medicine)
Jonathan Maltzman (University of Pennsylvania)
David Scadden (MGH)

(c) Employment and Research Opportunities

This award has provided salary support for technical personnel and for trainees in each of participating labs.

CONCLUSIONS

During the 10 year of its existence, this consortium achieved its two major goals. The first was to generate and characterize accurate mouse models of NF1 and NF2-associated tumors. These strains have been distributed freely and widely and form the backbone of much ongoing research in the NF field. We note that the Preclinical Drug Discovery Initiative of the Children's Tumor Foundation as a remarkable example of how strains of mice engineered by this consortium are being utilized in innovative ways to advance NF research and facilitate the testing of new treatments for the complications of NF1 and NF2. The second major accomplishment of this group was the use of these mouse models to make novel insights regarding how the *Nf1* and *Nf2* gene products regulate cellular processes such as survival, adhesion, proliferation, wound healing, self-renewal, and signal transduction and how these processes are perturbed in tumorigenesis. This work has appeared in top notch peer-reviewed journals such as *Nature, Cell, Cancer Cell*, and *Genes and Development.* Insights made by our group in mouse models have directly facilitated innovative clinical trials in human patients. The investigators will continue to collaborate closely and have shared expertise and reagents extensively in the years ahead.

REFERENCES

1. Brannan CI, Perkins AS, Vogel KS, Ratner N, Nordlund ML, Reid SW, et al. Targeted disruption of the neurofibromatosis type 1 gene leads to developmental abnormalities in heart and various neural crest-derived tissues. Genes and Development. 1994;8:1019-29.

2. Jacks T, Shih S, Schmitt EM, Bronson RT, Bernards A, Weinberg RA. Tumorigenic and developmental consequences of a targeted *Nf1* mutation in the mouse. Nat Genet. 1994;7:353-61.
3. Zhu Y, Romero MI, Ghosh P, Ye Z, Charnay P, Rushing EJ, et al. Ablation of NF1 function in neurons induces abnormal development of cerebral cortex and reactive gliosis in the brain. Genes Dev. 2001;15(7):859-76.
4. Giovannini M, Robanus-Maandag E, Niwa-Kawakita M, van der Valk M, Woodruff JM, Goutebroze L, et al. Schwann cell hyperplasia and tumors in transgenic mice expressing a naturally occurring mutant NF2 protein. Genes Dev. 1999;13(8):978-86.
5. McClatchey AI, Saotome I, Ramesh V, Gusella JF, Jacks T. The Nf2 tumor suppressor gene product is essential for extraembryonic development immediately prior to gastrulation. Genes Dev. 1997;11(10):1253-65.
6. Giovannini M, Robanus-Maandag E, van der Valk M, Niwa-Kawakita M, Abramowski V, Goutebroze L, et al. Conditional biallelic Nf2 mutation in the mouse promotes manifestations of human neurofibromatosis type 2. Genes Dev. 2000;14(13):1617-30.
7. Chao RC, Pyzel U, Fridlyand J, Kuo YM, Teel L, Haaga J, et al. Therapy-induced malignant neoplasms in Nf1 mutant mice. Cancer Cell. 2005 Oct;8(4):337-48.
8. Cichowski K, Shih TS, Schmitt E, Santiago S, Reilly K, McLaughlin ME, et al. Mouse models of tumor development in neurofibromatosis type 1. Science. 1999;286(5447):2172-6.
9. Mahgoub N, Taylor B, Le Beau M, Gratiot M, Carlson K, Jacks T, et al. Myeloid malignancies induced by alkylating agents in Nf1 mice. Blood. 1999;93:3617-23.
10. Mahgoub N, Taylor BR, Gratiot M, Kohl NE, Gibbs JB, Jacks T, et al. In vitro and In vivo effects of a farnesyltransferase inhibitor on Nf1- deficient hematopoietic cells. Blood. 1999;94(7):2469-76.
11. Reilly KM, Loisel DA, Bronson RT, McLaughlin ME, Jacks T. Nf1;Trp53 mutant mice develop glioblastoma with evidence of strain- specific effects. Nat Genet. 2000;26(1):109-13.
12. Zhu Y, Ghosh P, Charnay P, Burns DK, Parada LF. Neurofibromas in NF1: Schwann cell origin and role of tumor environment. Science. 2002;296(5569):920-2.
13. McLaughlin ME, Kruger GM, Slocum KL, Crowley D, Michaud NA, Huang J, et al. The Nf2 tumor suppressor regulates cell-cell adhesion during tissue fusion. Proc Natl Acad Sci U S A. 2007 Feb 27;104(9):3261-6.
14. Zhu Y, Harada T, Liu L, Lush ME, Guignard F, Harada C, et al. Inactivation of NF1 in CNS causes increased glial progenitor proliferation and optic glioma formation. Development. 2005 Dec;132(24):5577-88.
15. Bajenaru ML, Hernandez MR, Perry A, Zhu Y, Parada LF, Garbow JR, et al. Optic nerve glioma in mice requires astrocyte Nf1 gene inactivation and Nf1 brain heterozygosity. Cancer Res. 2003 Dec 15;63(24):8573-7.
16. Bajenaru ML, Zhu Y, Hedrick NM, Donahoe J, Parada LF, Gutmann DH. Astrocyte-specific inactivation of the neurofibromatosis 1 gene (NF1) is insufficient for astrocytoma formation. Mol Cell Biol. 2002 Jul;22(14):5100-13.
17. Mi H, Barres BA. Purification and characterization of astrocyte precursor cells in the developing rat optic nerve. J Neurosci. 1999 Feb 1;19(3):1049-61.
18. Wallace VA, Raff MC. A role for Sonic hedgehog in axon-to-astrocyte signalling in the rodent optic nerve. Development. 1999 July 1, 1999;126(13):2901-9.
19. Dahmane N, Sanchez P, Gitton Y, Palma V, Sun T, Beyna M, et al. The Sonic Hedgehog-Gli pathway regulates dorsal brain growth and tumorigenesis. Development. 2001 December 15, 2001;128(24):5201-12.

20. Chen JK, Taipale J, Cooper MK, Beachy PA. Inhibition of Hedgehog signaling by direct binding of cyclopamine to Smoothened. Genes and Development. 2002 November 1, 2002;16(21):2743-8.
21. Yang FC, Ingram DA, Chen S, Zhu Y, Yuan J, Li X, et al. Nf1-dependent tumors require a microenvironment containing Nf1+/-- and c-kit-dependent bone marrow. Cell. 2008 Oct 31;135(3):437-48.
22. Toma JG, Akhavan M, Fernandes KJ, Barnabe-Heider F, Sadikot A, Kaplan DR, et al. Isolation of multipotent adult stem cells from the dermis of mammalian skin. Nat Cell Biol. 2001 Sep;3(9):778-84.
23. McKenzie IA, Biernaskie J, Toma JG, Midha R, Miller FD. Skin-derived precursors generate myelinating Schwann cells for the injured and dysmyelinated nervous system. J Neurosci. 2006 Jun 14;26(24):6651-60.
24. Biernaskie JA, McKenzie IA, Toma JG, Miller FD. Isolation of skin-derived precursors (SKPs) and differentiation and enrichment of their Schwann cell progeny. Nat Protoc. 2006;1(6):2803-12.
25. Le LQ, Shipman T, Burns D, Parada LF. Cell of origin and microenvironment contribution for NF1-associated dermal neurofibromas. Cell Stem Cell. 2009;4(5):454-63
.
26. Asou H, Matsui H, Ozaki Y, Nagamachi A, Nakamura M, Aki D, et al. Identification of a common microdeletion cluster in 7q21.3 subband among patients with myeloid leukemia and myelodysplastic syndrome. Biochem Biophys Res Commun. 2009 May 29;383(2):245-51.
27. Yang FC, Ingram DA, Chen S, Hingtgen CM, Ratner N, Monk KR, et al. Neurofibromin-deficient Schwann cells secrete a potent migratory stimulus for Nf1+/- mast cells. J Clin Invest. 2003 Dec;112(12):1851-61.
28. Vogel KS, Klesse LJ, Velasco-Miguel S, Meyers K, Rushing EJ, Parada LF. Mouse tumor model for neurofibromatosis type 1. Science. 1999;286(5447):2176-9.
29. Maris JM, Wiersma SR, Mahgoub N, Thompson P, Geyer RJ, Lange BJ, et al. Monosomy 7 myelodysplastic syndrome and other second malignant neoplasms in children with neurofibromatosis type 1. Cancer. 1997;79:1438-46.
30. Sharif S, Ferner R, Birch JM, Gillespie JE, Gattamaneni HR, Baser ME, et al. Second primary tumors in neurofibromatosis 1 patients treated for optic glioma: substantial risks after radiotherapy. J Clin Oncol. 2006 Jun 1;24(16):2570-5.
31. Curto M, Cole BK, Lallemand D, Liu CH, McClatchey AI. Contact-dependent inhibition of EGFR signaling by Nf2/Merlin. J Cell Biol. 2007 Jun 4;177(5):893-903.
32. Cole BK, Curto M, Chan AW, McClatchey AI. Localization to the cortical cytoskeleton is necessary for Nf2/merlin-dependent epidermal growth factor receptor silencing. Mol Cell Biol. 2008 Feb;28(4):1274-84.
33. Lazar CS, Cresson CM, Lauffenburger DA, Gill GN. The Na+/H+ exchanger regulatory factor stabilizes epidermal growth factor receptors at the cell surface. Mol Biol Cell. 2004 Dec;15(12):5470-80.
34. McCartney BM, Kulikauskas RM, LaJeunesse DR, Fehon RG. The neurofibromatosis-2 homologue, Merlin, and the tumor suppressor expanded function together in Drosophila to regulate cell proliferation and differentiation. Development. 2000 Mar;127(6):1315-24.
35. Hamaratoglu F, Willecke M, Kango-Singh M, Nolo R, Hyun E, Tao C, et al. The tumour-suppressor genes NF2/Merlin and Expanded act through Hippo signalling to regulate cell proliferation and apoptosis. Nat Cell Biol. 2006 Jan;8(1):27-36.

36. Morris ZS, McClatchey AI. Aberrant epithelial morphology and persistent epidermal growth factor receptor signaling in a mouse model of renal carcinoma. Proc Natl Acad Sci U S A. 2009 Jun 16;106(24):9767-72.
37. Pietri T, Eder O, Blanche M, Thiery JP, Dufour S. The human tissue plasminogen activator-Cre mouse: a new tool for targeting specifically neural crest cells and their derivatives in vivo. Developmental biology. 2003 Jul 1;259(1):176-87.
38. Mantamadiotis T, Lemberger T, Bleckmann SC, Kern H, Kretz O, Martin Villalba A, et al. Disruption of CREB function in brain leads to neurodegeneration. Nat Genet. 2002 May;31(1):47-54.
39. Shaw R, Paez J, Curto M, Taktine A, Pruitt W, Sadtome I, et al. The neurofibromatosis type 2 tumor suppressor protein, merlin, functions in Rac-dependent signaling. Dev Cell. 2001;1:63-72.
40. Etienne-Manneville S, Hall A. Rho GTPases in cell biology. Nature. 2002 Dec 12;420(6916):629-35.
41. Lakkis MM, Golden JA, O'Shea KS, Epstein JA. Neurofibromin deficiency in mice causes exencephaly and is a modifier for Splotch neural tube defects. Developmental biology. 1999 Aug 1;212(1):80-92.
42. Creuzet SE, Martinez S, Le Douarin NM. The cephalic neural crest exerts a critical effect on forebrain and midbrain development. Proc Natl Acad Sci U S A. 2006 Sep 19;103(38):14033-8.
43. Lauchle JO, Kim D, Le DT, Akagi K, Crone M, Krisman K, et al. Response and resistance to MEK inhibition in leukaemias initiated by hyperactive Ras. Nature. 2009 Sep 17;461(7262):411-4.
44. Dupuy AJ, Akagi K, Largaespada DA, Copeland NG, Jenkins NA. Mammalian mutagenesis using a highly mobile somatic Sleeping Beauty transposon system. Nature. 2005 Jul 14;436(7048):221-6.